Import and fate of fluorescent analogs of oxidized phospholipids in vascular smooth muscle cells

Alexandra Moumtzi,[1,*] Michael Trenker,[1,*] Karlheinz Flicker,[*] Elfriede Zenzmaier,[*] Robert Saf,[†] and Albin Hermetter[2,*]

Institute of Biochemistry* and Institute for Chemistry and Technology of Organic Materials,† Graz University of Technology, A-8010 Graz, Austria

Abstract **Lipid oxidation is now thought to be an initiating and sustaining event in atherogenesis. Oxidatively fragmented phospholipids, namely 1-palmitoyl-2-glutaroyl-*sn*-glycero-3-phosphocholine (PGPC) and 1-palmitoyl-2-(5-oxovaleroyl)-*sn*-glycero-3-phosphocholine (POVPC), present in minimally modified LDL and atherosclerotic lesions, have been reported to elicit a wide range of pathophysiological responses in the cells of the vascular wall. Nevertheless, the question of their potential sites of action and their primary molecular targets remains open. To address this issue, a series of fluorescently labeled analogs, which differ with regard to structure and binding site of the fluorophore, were synthesized and used as tools for studying the uptake, intracellular stability, and distribution of PGPC and POVPC in vascular smooth muscle cells (VSMCs). We demonstrate that in accordance with their lysophospholipid-like structure, these highly similar molecules transferred rapidly either from aqueous phospholipid dispersions or preloaded native LDL into VSMCs, producing disparate fluorescence patterns irrespective of the attached fluorophore. PGPC derivatives were translocated to the lysosomes. In sharp contrast, POVPC analogs were initially captured in the plasma membrane, most likely in consequence of the formation of covalent adducts with free amino and sulfhydryl groups of proteins and phospholipids. LDL internalization is not required for cellular lipid uptake. Collectively, our data provide evidence that oxidized phospholipids, owing to their high exchangeability between lipoproteins and cell membranes, may act within a short time on different cellular sites in VSMCs and affect various lipid and protein components through physical or chemical interactions, which might then serve as starting points for intracellular signaling.**—Moumtzi, A., M. Trenker, K. Flicker, E. Zenzmaier, R. Saf, and A. Hermetter. **Import and fate of fluorescent analogs of oxidized phospholipids in vascular smooth muscle cells.** ***J. Lipid Res.*** **2007.** 48: **565–582.**

Supplementary key words atherosclerosis • lipoproteins • lipid synthesis • lipid transport

Oxidative modification of LDL is considered an important pathogenetic factor in atherosclerosis (1–3). Preferential targets of oxidative attack are the esterified polyunsaturated fatty acids in the phospholipids of biological membranes and the shell that surrounds the insoluble lipids of lipoproteins (4). Oxidative fragmentation of arachidonoyl phospholipids results in shortened *sn*-2 residues with or without ω-aldehydic, ω-hydroxy, or ω-carboxy functions (5, 6). Such compounds are also formed in vitro by oxidation of 1-palmitoyl-2-arachidonoyl-*sn*-glycero-3-phosphocholine (7, 8). It has been demonstrated that the truncated *sn*-2 substituents of these compounds are major determinants of their bioactivity (9). Studies from several laboratories have revealed that the biological effects triggered by minimally modified LDL can largely be attributed to phospholipid oxidation products (7, 8, 10, 11). Their increased levels in atherosclerotic plaques (12, 13) and the increased antibody titers against oxidized phospholipids in humans and mice with lesions (14–16) attract attention to the pathological relevance of these molecules.

A rapidly growing interest has been focused on two major representatives in the series of homologous oxidized phospholipids, namely 1-palmitoyl-2-glutaroyl-*sn*-glycero-3-phosphocholine (PGPC) and 1-palmitoyl-2-(5-oxovaleroyl)-*sn*-glycero-3-phosphocholine (POVPC). Their importance is stressed by the finding that they selectively activate processes in vascular cells that may contribute to the path-

Abbreviations: AcOH, acetic acid; Alexa647, Alexa Fluor 647; apoB, apolipoprotein B-100; BODIPY, 4,4-difluoro-4-bora-3a,4a-diaza-*s*-indacene; 2-D, two-dimensional; DCC, *N,N′*-dicyclohexylcarbodiimide; DMAP, *p*-(*N,N*-dimethylamino)pyridine; ER, endoplasmic reticulum; EtOH, ethanol; FCS, fetal calf serum; HNE, 4-hydroxy-2-nonenal; MALDI-TOF, matrix-assisted laser desorption/ionization time-of-flight; MeOH, methanol; PGPC, 1-palmitoyl-2-glutaroyl-*sn*-glycero-3-phosphocholine; PGPE, 1-palmitoyl-2-glutaroyl-*sn*-glycero-3-phosphoethanolamine; PLA_2, phospholipase A_2; PLD, phospholipase D; POPE, 1-palmitoyl-2-oleoyl-*sn*-glycero-3-phosphoethanolamine; POVPC, 1-palmitoyl-2-(5-oxovaleroyl)-*sn*-glycero-3-phosphocholine; POVPE, 1-palmitoyl-2-(5-oxovaleroyl)-*sn*-glycero-3-phosphoethanolamine; PyrGPC, 1-(10-pyrenedecanoyl)-2-glutaroyl-*sn*-glycero-3-phosphocholine; PyrOPC, 1-(10-pyrenedecanoyl)-2-oleoyl-*sn*-glycero-3-phosphocholine; PyrOVPC, 1-(10-pyrenedecanoyl)-2-(5-oxovaleroyl)-*sn*-glycero-3-phosphocholine; R_f, relative mobility; SE, succinimidyl ester; VSMC, vascular smooth muscle cell.

[1] A. Moumtzi and M. Trenker contributed equally to this work.
[2] To whom correspondence should be addressed.
e-mail: albin.hermetter@tugraz.at

Manuscript received 1 February 2006 and in revised form 29 November 2006.
Published, JLR Papers in Press, November 29, 2006.
DOI 10.1194/jlr.M600394-JLR200

Copyright © 2007 by the American Society for Biochemistry and Molecular Biology, Inc.
This article is available online at http://www.jlr.org

Downloaded from www.jlr.org by guest, on June 14, 2012

ogenesis of atherosclerosis as well as other chronic inflammatory diseases. It is noteworthy that, in spite of their high structural similarity, due to a single hydrophobic chain, a bulky polar head group, and the polar *sn*-2 acyl fragment, they partially exert different cellular effects. PGPC and POVPC exhibit proinflammatory actions (7, 17–19) but also increase the synthesis of protective enzymes such as heme oxygenase 1 (20). In human vascular smooth muscle cells (VSMCs), POVPC and, to a lesser extent, PGPC activated apoptotic signaling pathways via the stimulation of acid sphingomyelinase (11).

VSMCs can acquire a broad spectrum of different phenotypes in response to changes in a variety of physiological or pathological factors (21, 22), including oxidized phospholipids (11, 18, 23). Nonetheless, the primary molecular targets and the mechanisms of their activation by these molecules are largely unknown. The identification of the cell compartments that accumulate oxidized phospholipids is of great importance in defining the mode of action by which they cause cellular dysfunction.

This study was designed to gain insight into the import, intracellular distribution, and potential targets of PGPC and POVPC in VSMCs. For this purpose, we synthesized different fluorescent analogs of the oxidized phospholipids. Using fluorescence microscopy, we found rapid uptake of both phospholipid species but substantial differences with regard to their intracellular accumulation. PGPC derivatives were initially transferred to perinuclear regions, corresponding to lysosomes and partially to the endoplasmic reticulum (ER), whereas labeled POVPC became highly enriched in the plasma membrane at early time points. These data support the assumption that multiple protein and lipid interaction sites must exist in VSMCs that are affected soon after their initial contact with oxidized phospholipids, thus initiating intracellular signaling.

EXPERIMENTAL PROCEDURES

Materials

Chemicals for lipid synthesis, *N,N′*-dicyclohexylcarbodiimide (DCC; purity > 98%), *p*-(*N,N*-dimethylamino)pyridine (DMAP; 99%), phospholipase A_2 (PLA_2) from *Naja naja* venom in Tris buffer (pH 8.9) (EC 3.1.1.4; specific activity, 1,000 IU/mg), and phospholipase D (PLD) type VII from *Streptomyces* species in Tris buffer (pH 5.6) (EC 3.1.4.4; specific activity, 500 IU/mg) were obtained from Sigma-Aldrich. 4,4-Difluoro-4-bora-3a,4a-diaza-*s*-indacene-succinimidyl ester (BODIPY™SE), Alexa™ Fluor 647 (Alexa647)-SE, and 1-pyrenedecanoic acid were purchased from Molecular Probes (Eugene, OR). Chemicals for gel electrophoresis were from Bio-Rad Laboratories (Hercules, CA), unless noted otherwise. The dye reagent for the Bradford protein assay was also purchased from Bio-Rad. Organic solvents and all other reagents were obtained from Merck (Darmstadt, Germany), unless indicated otherwise. Tissue culture dishes and flasks were obtained from Sarstedt (Nürmbrecht, Germany). Media and supplements for cell culture were purchased from PAA Laboratories (Linz, Austria). Ninety-six-well microtiter plates for protein determinations were obtained from Greiner (Kremsmünster, Austria).

Cell culture

Rat aortic smooth muscle cells (A7r5; catalog No. CRL-1444, smooth muscle, thoracic aorta, DBIX rat; American Type Culture Collection, Rockville, MD) were cultivated in DMEM supplemented with 10% fetal calf serum (FCS), 2 mM L-glutamine, 100 U/ml penicillin/streptomycin, and 25 mM HEPES at 37°C in a humidified CO_2 (8%) atmosphere. Incubations with fluorescent phospholipids were routinely carried out in serum-free culture medium at 37°C in a CO_2 incubator after washing cells twice with PBS to remove residual FCS. Working solutions of the labeled lipids were prepared by diluting dispersions of these compounds in PBS with the appropriate amount of incubation medium.

Synthesis of aliphatic and fluorescent phospholipids

TLC was routinely performed on aluminum plates precoated with 0.25 mm of silica gel 60 (Merck, Darmstadt, Germany). $CHCl_3$/methanol (MeOH)/water (65:25:4, v/v/v) was used as the developing system, unless indicated otherwise. Spots were visualized by illumination under short-wavelength ultraviolet light (fluorophores) or by treatment with molybdenum blue reagent (phosphorus) (24), 50% H_2SO_4 (organic material), or ninhydrin (amino groups). Anhydrous dichloromethane was obtained by distillation over phosphorus pentoxide. Flash column chromatography was performed on 230–400 mesh silica gel supplied by Merck. Fluorescence spectroscopic measurements of methanolic solutions of the fluorescent phospholipids were conducted in quartz cuvettes using a spectrofluorophotometer (RF-3501 PC; Shimadzu, Korneuburg, Austria). The concentrations and quantities of lipids were determined by phosphorus analysis (25) or by absorption measurements of the fluorescent compounds.

Synthesis of PGPC

PGPC (**Fig. 1A**, compound 1) was synthesized according to a modified version of the procedure of Watson et al. (12) and Subbanagounder, Watson, and Berliner (26). A solution of dry 1-palmitoyl-*sn*-glycero-3-phosphocholine (62 mg, 125 μmol), dry glutaric anhydride (70 mg, 613 μmol, 5 eq), and DMAP (75 mg, 614 μmol, 5 eq) in 6 ml of anhydrous dichloromethane was magnetically stirred overnight at 35°C. The reaction was monitored by TLC with $CHCl_3$/MeOH/25% NH_3 (65:35:5, v/v/v) as a developing system and quenched by the addition of 3 ml of MeOH. The resulting mixture was washed once with 1.8 ml of MeOH/water (1:1, v/v). After evaporation of the organic phase, excess DMAP was removed by trituration with 4 ml of diethylether. Removal of the supernatant gave 32 mg of PGPC [42%; relative mobility (R_f) = 0.05].

Synthesis of 1-palmitoyl-2-glutaroyl-*sn*-glycero-3-phosphoethanolamine

1-Palmitoyl-2-glutaroyl-*sn*-glycero-3-phosphoethanolamine (PGPE) (Fig. 1A, compound 2) was obtained by transphosphatidylation of PGPC (90 mg, 148 μmol) (Fig. 1A, compound 1) by PLD (29 units) in an emulsion of 1.4 ml of toluene and 4.3 ml of a 0.5 M sodium acetate buffer (pH 7.2) containing 0.5 M ethanolamine (Fig. 1A, step 1). The biphasic system was stirred at 35°C overnight. The reaction was monitored by TLC and quenched by the addition of 4.3 ml of MeOH. The product was extracted with 43 ml of $CHCl_3$/MeOH (2:1, v/v). The organic phase was washed twice with 11 ml of MeOH/water (1:1, v/v) to remove excess ethanolamine, evaporated, and subjected to preparative TLC. The product was scraped off and eluted three times from the silica gel with $CHCl_3$/MeOH (1:4, v/v). Evaporation of the combined extracts yielded the desired product (30.3 mg, 36%; R_f = 0.30).

Downloaded from www.jlr.org by guest, on June 14, 2012

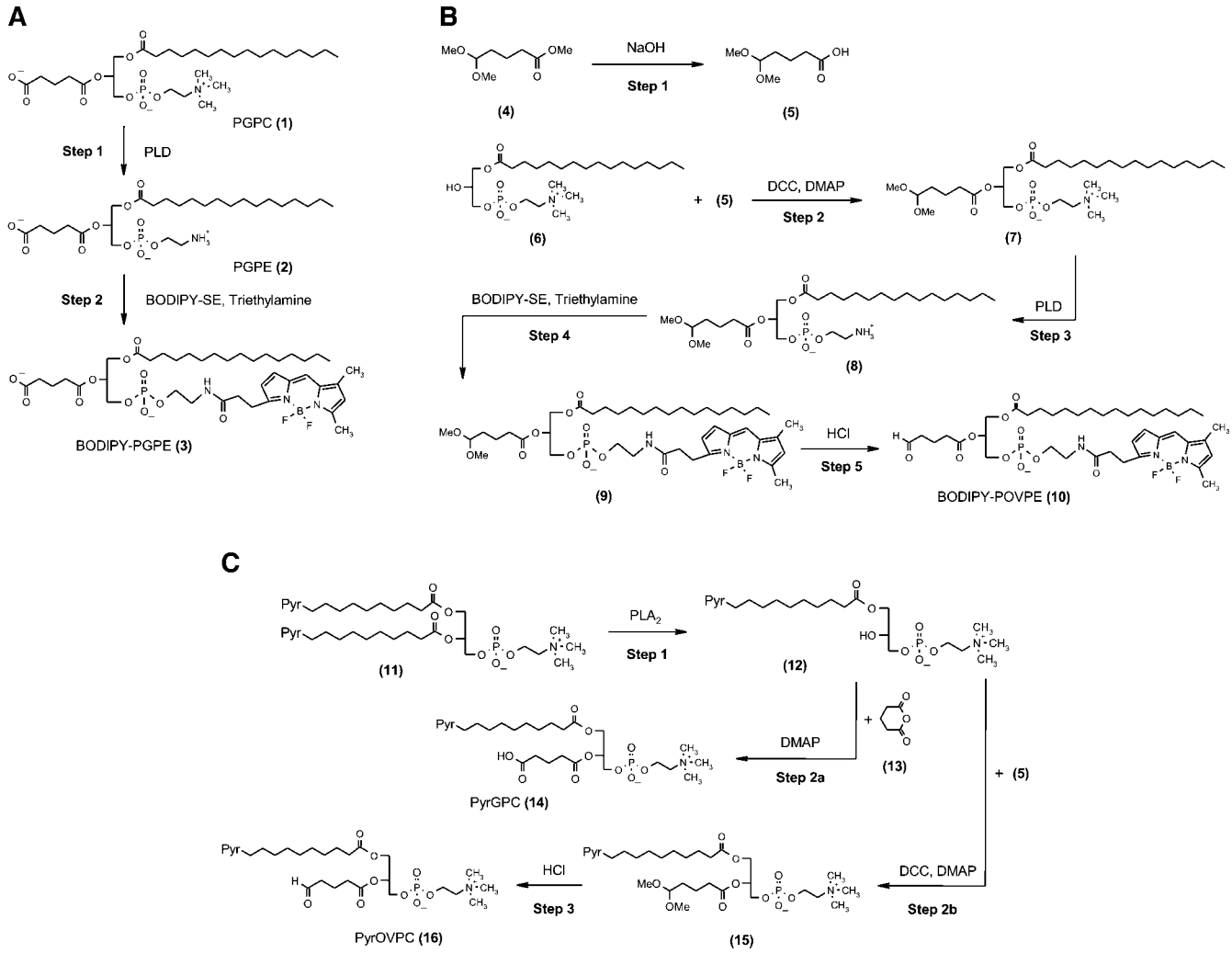

Fig. 1. Syntheses of 4,4-difluoro-4-bora-3a,4a-diaza-*s*-indacene (BODIPY) and pyrene analogs of 1-palmitoyl-2-glutaroyl-*sn*-glycero-3-phosphocholine (PGPC) and 1-palmitoyl-2-(5-oxovaleroyl)-*sn*-glycero-3-phosphocholine (BODIPY-POVPC). A: BODIPY-1-palmitoyl-2-glutaroyl-*sn*-glycero-3-phosphoethanolamine (BODIPY-PGPE). B: BODIPY-1-palmitoyl-2-(5-oxovaleroyl)-*sn*-glycero-3-phosphoethanolamine (POVPE). C: 1-(10-Pyrenedecanoyl)-2-glutaroyl-*sn*-glycero-3-phosphocholine (PyrGPC) and 1-(10-pyrenedecanoyl)-2-(5-oxovaleroyl)-*sn*-glycero-3-phosphocholine (PyrOVPC). DCC, *N,N′*-dicyclohexylcarbodiimide; DMAP, *p*-(*N,N*-dimethylamino)pyridine; PLA_2, phospholipase A_2; PLD, phospholipase D; SE, succinimidyl ester.

Synthesis of BODIPY-PGPE

To a magnetically stirred solution of BODIPY-SE (0.96 mg, 2.5 μmol) in 1 ml of $CHCl_3$/MeOH (2:1, v/v) were added PGPE (4.4 mg, 7.8 μmol, 3 eq) (Fig. 1A, compound 2) and triethylamine pro analysi (p.a.) (10 μl, 72 μmol, 30 eq) (Fig. 1A, step 2). Then the flask was flushed with nitrogen and protected from light, and the resulting solution was stirred at room temperature for 1 h. The progress of the reaction was monitored by TLC. The solvent was removed under a nitrogen stream until a volume of 400 μl was reached, from which the lipid was purified by preparative TLC. The desired compound was visualized under ultraviolet light, scraped off the TLC plate, and eluted three times from the silica gel with $CHCl_3$/MeOH (1:4, v/v). The solvent was removed from the combined extracts by rotary evaporation to give BODIPY-PGPE (1.77 mg, 85%; R_f = 0.28) (Fig. 1A, compound 3).

Synthesis of Alexa647-PGPE

Alexa647-PGPE corresponds to BODIPY-PGPE (Fig. 1A, compound 3) but contains Alexa647 instead of BODIPY on its head group. It was obtained from Alexa647-SE (0.5 mg, 0.4 μmol) and PGPE (0.68 mg, 1.2 μmol, 3 eq) (Fig. 1A, compound 2) in 0.5 ml of $CHCl_3$/MeOH (2:1, v/v) after the addition of triethylamine p.a. (5 μl, 36 μmol, 90 eq) followed by stirring at room temperature for 90 min. The reaction mixture was strictly protected from light. The progress of the reaction was monitored by TLC (RP-18 F_{254s}; Merck). The product was purified by preparative TLC with water/ethanol (EtOH)/*n*-propanol (20:57:23, v/v/v) as a developing system, scraped off, and eluted twice with $CHCl_3$/MeOH (1:1, v/v) and once with MeOH. Removal of the solvent under a stream of nitrogen gave Alexa647-PGPE (0.26 μmol, 65%; R_f = 0.80).

Synthesis of 1-palmitoyl-2-(5-dimethoxypentanoyl)-*sn*-glycero-3-phosphoethanolamine

A solution of 5,5-dimethoxypentanoic acid methyl ester (220 mg, 1.25 mmol) (Fig. 1B, compound 4) and sodium hydroxide (250 mg, 6.25 mmol, 5 eq) in 5 ml of water/MeOH/tetrahydrofuran (2:5:3, v/v/v) was stirred at room temperature for 90 min (Fig. 1B, step 1). After cooling to 0°C, the reaction

Downloaded from www.jlr.org by guest, on June 14, 2012

mixture was acidified to pH 2.1 by subsequent addition of 6 ml of 1 N HCl and appropriate amounts of 0.1 N HCl and then extracted with dichloromethane (3 × 15 ml). The combined organic extracts were washed with water (2 × 10 ml) and dried over Na_2SO_4. The solvent was removed under reduced pressure except for 10–15 ml containing the desired product ($R_f = 0.35$) (Fig. 1B, compound 5), which was immediately used for the acylation reaction without further purification. 1-Palmitoyl-*sn*-glycero-3-phosphocholine (209 mg, 0.42 mmol) (Fig. 1B, compound 6), DCC (270 mg, 1.3 mmol, 3 eq), and DMAP (160 mg, 1.3 mmol, 3 eq) were added to this solution of 5,5-dimethoxypentanoic acid (Fig. 1B, step 2). The mixture was stirred under nitrogen at room temperature overnight. The reaction was monitored by TLC. After the addition of 6 ml of MeOH, the organic solution was washed twice with MeOH/water (1:1, v/v). The solvent was removed under vacuum, and traces of water were evaporated after the addition of benzene/EtOH (3:2, v/v). The oily residue was flash chromatographed on 12 g of silica gel with $CHCl_3$/MeOH/25% NH_3 (65:35:5, v/v/v) as a solvent to give 1-palmitoyl-2-(5,5-dimethoxypentanoyl)-*sn*-glycero-3-phosphocholine (245 mg, 91%; $R_f = 0.14$) (Fig. 1B, compound 7). The ethanolamine analog (Fig. 1B, compound 8) was obtained by transphosphatidylation of the choline lipid as described previously for the conversion of PGPC to PGPE (compare Fig. 1A, step 1) [yield, 6.2 mg, 66%; $R_f = 0.24$ using $CHCl_3$/MeOH/25% NH_3 (65:35:5, v/v/v) as a developing solvent] (Fig. 1B, step 3).

Synthesis of 1-palmitoyl-2-(5-oxovaleroyl)-*sn*-glycero-3-phospho-*N*-(3-BODIPY-propionyl)-ethanolamine

Triethylamine p.a. (10 μl, 72 μmol, 14 eq) was added to a solution of 1-palmitoyl-2-(5,5-dimethoxypentanoyl)-*sn*-glycero-3-phosphoethanolamine (3.0 mg, 5.0 μmol) (Fig. 1B, compound 8) and BODIPY-SE (1.95 mg, 5.0 μmol, 1 eq) in 1 ml of $CHCl_3$/MeOH (2:1, v/v) (Fig. 1B, step 4). The reaction mixture was stirred at room temperature for 80 min. The solvent was removed under vacuum, yielding 1-palmitoyl-2-(5,5-dimethoxypentanoyl)-*sn*-glycero-3-phospho-*N*-(3-BODIPY-propionyl)-ethanolamine (Fig. 1B, compound 9), which was suitable for the next reaction without further purification. Release of the desired product was accomplished by acetal cleavage of this stable precursor (2.0 mg, 2.3 μmol) with 400 μl of tetrahydrofuran-HCl (1 N) (Fig. 1B, step 5). After only 2 min, the reaction mixture was neutralized with $NaHCO_3$ followed by extraction of the product with 1.2 ml of $CHCl_3$/MeOH (2:1, v/v). The organic phase was washed twice with 300 μl of water, dried over Na_2SO_4, and evaporated under reduced pressure, leading to 1.65 mg of BODIPY-1-palmitoyl-2-(5-oxovaleroyl)-*sn*-glycero-3-phosphoethanolamine (POVPE) [87%; $R_f = 0.22$ using $CHCl_3$/MeOH/water (15:5:0.1, v/v/v) as a developing system] (Fig. 1B, compound 10).

Synthesis of 1-palmitoyl-2-oleoyl-*sn*-glycero-3-phospho-*N*-(3-BODIPY-propionyl)-ethanolamine

BODIPY-SE (1.00 mg, 2.57 μmol), triethylamine p.a. (10 μl, 72 μmol, 28 eq), and 1-palmitoyl-2-oleoyl-*sn*-glycero-3-phosphoethanolamine (POPE; 5.53 mg, 7.70 μmol, 3 eq) were dissolved in 1 ml of $CHCl_3$/MeOH (2:1, v/v). The mixture was stirred at room temperature for 60 min, and the solvent was removed under a stream of nitrogen. The white oily residue was dissolved in 500 μl of $CHCl_3$/MeOH (2:1, v/v). The product was purified by preparative TLC. The fluorescent band containing the product was scraped off the plate and eluted three times with $CHCl_3$/MeOH (1:4, v/v). The combined extracts were evaporated to deliver the desired product (1.31 mg, 51%; $R_f = 0.59$).

Synthesis of 1-(10-pyrenedecanoyl)-2-glutaroyl-*sn*-glycero-3-phosphocholine

To a magnetically stirred emulsion of 1,2-bis(10-pyrenedecanoyl)-*sn*-glycero-3-phosphocholine (45 mg, 47 μmol) (Fig. 1C, compound 11) in a mixture of 3 ml of 0.1 M Tris-HCl buffer (pH 8) containing 0.1 M $CaCl_2$ and 3 ml of diethylether (peroxide-free) were added 50 units of PLA_2 (*Naja naja* venom) (Fig. 1C, step 1). The reaction mixture was stirred overnight at 35–40°C. After removing the diethylether, the product was extracted from the aqueous solution with $CHCl_3$/MeOH (2:1, v/v) (3 × 5 ml). The combined organic fractions were evaporated and the residual water was removed under high vacuum, leading to 50 mg of a mixture of 1-(10-pyrenedecanoyl)-*sn*-glycero-3-phosphocholine (Fig. 1C, compound 12) and free pyrenedecanoic acid. The latter compound was removed by trituration with diethylether. After removal of the solvent under vacuum, 25 mg of the pure lysophospholipid was obtained [88%; $R_f = 0.12$ in $CHCl_3$/MeOH/AcOH/water (50:30:10:5, v/v/v/v) as a developing system]. Glutaric anhydride (12 mg, 105 μmol, 11 eq) and anhydrous DMAP (4 mg, 33 μmol, 3 eq) were added to a solution of the lysophospholipid (6.0 mg, 9.8 μmol) in 3 ml of anhydrous dichloromethane (Fig. 1C, step 2a). The reaction was stirred overnight at 35–40°C. Flash chromatography of the crude product on 10 g of silica gel with $CHCl_3$/MeOH/water (65:25:4, v/v/v) led to 1-(10-pyrenedecanoyl)-2-glutaroyl-*sn*-glycero-3-phosphocholine (PyrGPC) [2.2 mg, 31%; $R_f = 0.18$ in $CHCl_3$/MeOH/AcOH/water (50:30:10:5, v/v/v/v) as a developing system] (Fig. 1C, compound 14).

Synthesis of 1-(10-pyrenedecanoyl)-2-(5-oxovaleroyl)-*sn*-glycero-3-phosphocholine

1-(10-Pyrenedecanoyl)-*sn*-glycero-3-phosphocholine (10 mg, 16 μmol) (Fig. 1C, compound 12) was acylated with compound 5 in 10 ml of dichloromethane containing DCC (200 mg, 1.0 mmol, 59 eq) and DMAP (200 mg, 1.6 mmol, 100 eq). The reaction mixture was stirred at room temperature overnight (Fig. 1C, step 2b). The progress of the reaction was monitored by TLC until the reaction was stopped by the addition of 6 ml of MeOH. The resultant solution was washed twice with MeOH/water (1:1, v/v), and the solvent was removed under reduced pressure. The crude product was purified by preparative TLC, scraped off, and eluted five times with 4 ml of $CHCl_3$/MeOH (1:4, v/v). Residual silica gel was removed by washing the combined organic fractions (concentrated to a volume of 5 ml) with 1 ml of MeOH/water (1:1, v/v). Evaporation of the solvent yielded 6 mg of 1-(10-pyrenedecanoyl)-2-(5,5-dimethoxypentanoyl)-*sn*-glycero-3-phosphocholine (49%; $R_f = 0.17$) (Fig. 1C, compound 15). Deprotection of compound 15 (5.6 mg, 7.4 μmol) was performed in analogy to the acid-catalyzed hydrolysis of compound 9 (compare Fig. 1B, step 5), producing 1.1 mg of 1-(10-pyrenedecanoyl)-2-(5-oxovaleroyl)-*sn*-glycero-3-phosphocholine (PyrOVPC) (21%; $R_f = 0.05$) (Fig. 1C, step 3).

Synthesis of 1-(10-pyrenedecanoyl)-2-oleoyl-*sn*-glycero-3-phosphocholine

Oleic acid (99%) (10 μl, 28 μmol, 3 eq), anhydrous DCC (15 mg, 73 μmol, 9 eq), and DMAP (15 mg, 123 μmol, 15 eq) were added to a solution of compound 12 (5.0 mg, 8.2 μmol) in 3 ml of anhydrous dichloromethane. The mixture was stirred at room temperature overnight. The product was purified by preparative TLC. The fluorescent band containing the product was scraped off the plate and eluted three times with $CHCl_3$/MeOH (1:4, v/v). The combined extracts were evaporated to deliver pure 1-(10-pyrenedecanoyl)-2-oleoyl-*sn*-glycero-3-phosphocholine (PyrOPC) (3.68 mg, 51%; $R_f = 0.13$).

Downloaded from www.jlr.org by guest, on June 14, 2012

Mass spectrometry

Matrix-assisted laser desorption/ionization time-of-flight (MALDI-TOF) mass spectrometry was performed on a Micromass TofSpec2E apparatus equipped with a nitrogen laser (λ = 337 nm, operated at 5 Hz) and a time-lag focusing unit. Ions were generated by irradiation just above the threshold laser power. The spectra were recorded in the reflectron mode with an acceleration voltage of 20 kV and externally calibrated with a suitable mixture of poly(ethylene glycol)s. Samples were typically prepared by mixing solutions of the matrix (2,5-dihydroxybenzoic acid; concentration = 10 mg/ml, CH_3CN/0.1% trifluoroacetic acid, 70:30, v/v), the analyte (c = 0.01–1 mg/ml, $CHCl_3$/MeOH, 2:1, v/v), and Na-trifluoroacetic acid (c = 1 mg/ml, CH_3CN/water, 70:30, v/v) in a ratio of 10:1:0.5 (v/v/v). A 0.5 μl aliquot of the mixture was deposited on the sample plate (stainless steel) and allowed to dry under air. The spectra of 50–100 shots were averaged to improve the signal-to-noise ratio. All *m/z* values discussed in this work correspond to the most intense peak of any isotope distribution.

Isolation, labeling, and enrichment of LDL with fluorescent phospholipids

Human LDL (1.019–1.069 g/ml) was isolated from pooled fresh plasma of normal individuals by density ultracentrifugation as described (27), filter-sterilized, and stored at 4°C until use within 1 week of isolation. Lipoprotein concentration is expressed in terms of protein content, which was measured by the method of Lowry et al. (28). Lipoprotein labeling with BODIPY-SE was performed as reported previously by Hofer et al. (29). For LDL loading with fluorescent phospholipids, 750 nmol of PyrGPC or 1.25 μmol of PyrOVPC was solubilized in $CHCl_3$/MeOH (2:1, v/v) and transferred into a pyrex tube. After removing the solvent under a stream of nitrogen, the dry lipid film was overlaid with 250 μg of LDL protein in 190 μl of PBS, dispersed by gentle agitation, and incubated for 30 min at room temperature under nitrogen in the dark. The resulting solution was adjusted to 5 ml with serum-free cell culture medium, leading to a final concentration of 50 μg protein/ml for LDL, 3 nmol/μg protein for PyrGPC, and 5 nmol/μg protein for PyrOVPC.

Fluorescence microscopy

For microscopy experiments, monolayer cultures of A7r5 cells were grown to low confluence in 60 mm Petri dishes containing three coverslips each. Phospholipid concentrations in serum-free culture medium depended on fluorophore emission intensities, individual uptake rates, and the capabilities of the technical equipment.

Import of lipids into cells. Experiments were performed with concentrations ranging from 0.1 μM for the BODIPY analogs and Alexa647-PGPE, to 0.5 μM particularly for BODIPY-POVPE, and to 2.0 μM for all pyrene derivatives. Incubation times were: 5, 15, 30, 45, 60, and 90 min (37°C). After treatment, cells were carefully rinsed with PBS and observed with an Axiovert 35 inverted fluorescence microscope equipped with a 100 × 1.3 numerical aperture Plan-Neofluar objective (Carl Zeiss, Oberkochen, Germany), a mercury-arc lamp (HBO® 50W/AC; OSRAM, Munich, Germany), and a Peltier-cooled scientific charge-coupled device digital camera system (AxioCam HR) driven by the AxioVision 3.0.6.36 software package (Carl Zeiss Vision GmbH). **Table 1** summarizes the filter sets used. Unlabeled cells were used to examine autofluorescence. For comparative studies, all photomicrographs in a series of experiments were taken and processed under identical conditions for a given fluorophore.

To determine the role of lipoprotein-cell interactions in the import and intracellular distribution of the fluorescent oxidized phospholipids, A7r5 cultures were incubated for 15 and 45 min at 37°C with LDL (50 μg protein/ml; total sample volume, 5 ml), either BODIPY-labeled or unlabeled, that had been preloaded with PyrGPC (3 nmol/μg protein) or PyrOVPC (5 nmol/μg protein). After incubation, cells were washed with PBS and viewed with the fluorescence microscope. Separate images were acquired for both labels. Filter sets and exposure times for these double-label experiments were selected such that there was hardly any crossover between BODIPY and the less intense pyrene fluorescence.

Colocalization experiments. Colocalization experiments were conducted using a Nikon inverted microscope (Eclipse 300TE; Nikon, Vienna, Austria) equipped with a CFI Plan Fluor 40× oil-immersion objective (numerical aperture 1.3; Nikon), an epifluorescence system (150W XBO; Optiquip, Highland Mills, NY), a computer-controlled z-stage (Ludl Electronic Products, Hawthorne, NY), and a liquid-cooled charge-coupled device camera (−30°C; Quantix KAF1400G2; Roper Scientific, Acton, MA). Image resolution was 0.171 μm/pixel. Excitation wavelengths were selected using a computer-controlled filter wheel (Ludl Electronic Products). Deconvolution imaging was performed using ImagePro 3.0 software (Media Cybernetics, Silver Spring, MD). For image analysis and two-dimensional (2-D) deconvolution, Metamorph 6.0 (Universal Imaging, Visitron Systems, Puchheim, Germany) was used.

To identify the compartment that accumulates BODIPY-PGPE, we stained cells for 30 min with three specific organelle markers: a lysosomal marker (LysoTracker Blue DND-22; 160 nM), an ER-Tracker (ER-Tracker Blue-White DPX; 200 nM), or a mitochondrion-selective probe (MitoTracker Red CMXRos; 200 nM), in serum-free culture medium followed by two washing steps with PBS and treatment with 10 nM BODIPY-PGPE for 15 min at 37°C. After rinsing the cells twice with PBS, the coverslip was transferred into an observation chamber and viewed with the fluorescence microscope.

TABLE 1. Excitation/emission maxima of fluorophores, and optical instrument settings for epifluorescence microscopy of these probes

	Wavelength		Fluorescence Microscope		
Fluorophore	Excitation Maxima	Emission Maxima	Excitation Filter	Beam Splitter	Barrier Filter
Pyrene	342	376	BP 353-377	395	LP 397
BODIPY	505	510	BP 450-490	510	LP 520
Alexa647	651[a]	671[a]	BP 575-625	645	BP 660-710

Alexa647, Alexa Fluor 647; BODIPY, 4,4-difluoro-4-bora-3a,4a-diaza-*s*-indacene. Fluorescently labeled phospholipids were dissolved in methanol to a concentration of 0.1 nM for the BODIPY analogs and 0.5 nM for the pyrene derivatives. No differences were observed between the spectral properties of either BODIPY- or pyrene-labeled samples. All numerical values represent wavelengths in nm.

[a] In methanol, as specified by the manufacturer.

Downloaded from www.jlr.org by guest, on June 14, 2012

Colocalization studies with BODIPY-POVPE were performed with FM 1-43 membrane probe, which is believed to insert into the outer leaflet of the cell membrane, where it becomes intensely fluorescent. For this purpose, cells were first incubated with 10 nM BODIPY-POVPE for 15 min at 37°C. After a double washing step with PBS, the fluorescence pattern of the labeled phospholipid was imaged in an observation chamber with the fluorescence microscope. Removal of the incubation medium was followed by treatment of the same cells with 150 nM FM 1-43 in prewarmed supplemented DMEM without FCS for 30 min. Finally, cells were thoroughly rinsed with PBS and additional images were acquired from the same subpopulation described above.

For visualization, cells were illuminated at 485 nm (485DF15; Omega Optical), 380 nm (380HT15; Omega Optical), and 575 nm (575DF25; Omega Optical). Emission was monitored at 535 nm (535WB40; Omega Optical) for the BODIPY phospholipids, at 633 nm (528-633DBEM; dichroic XF53; Omega Optical) for the MitoTracker and FM 1-43, and at 510 nm (510WB40; Omega Optical) for the LysoTracker and ER-Tracker.

After staining with the ER-Tracker and LysoTracker, the viability of cells was assessed using 5 μM YO-PRO-1 iodide (Molecular Probes) in serum-free culture medium for 10 min at room temperature. Cytotoxic effects were not observed with these organelle trackers or under the influence of 0.1 μM BODIPY-PGPE at 37°C for 1 h. YO-PRO-1 fluorescence was viewed with identical microscope settings as for BODIPY.

Labeling of cell proteins with BODIPY-POVPE

For each experiment, a fully confluent monolayer of A7r5 cells in one Petri dish (100 mm) was incubated in the dark for 30 min with 8 ml of a 2.5 μM BODIPY-POVPE dispersion in PBS supplemented with 100 mg/l $CaCl_2$ and 100 mg/l $MgCl_2 \cdot 6H_2O$. After treatment, cells were washed twice with ice-cold PBS and then scraped into 3 ml of PBS supplemented with 100 mg/l $CaCl_2$, 100 mg/l $MgCl_2 \cdot 6H_2O$, 1 mM PMSF, and 50 μM $NaCNBH_3$. The following steps were performed at 4°C. Cells were pelleted at 300 *g* for 3 min followed by lysis in 150 μl of neutral cell lysis buffer (20 mM HEPES, 2 mM EDTA, 1% Triton X-100, pH 7.4, 50 μM $NaCNBH_3$, 5 mM DTT, 1 mM PMSF for 1 h on ice; stock solutions of soybean trypsin inhibitor and leupeptin were added directly before use to adjust a final concentration of 10 μg/ml). The suspension was shaken vigorously every 15 min. To remove nuclei and cytoskeleton, the lysate was centrifuged at 1,000 *g* and 4°C for 5 min. A 1 mM solution of $NaCNBH_3$ in water was added to the supernatant to reach a final concentration of 100 μM. After reduction of formed Schiff bases at 37°C for 2 h, samples were stored at −20°C. Measurements of cell protein content were performed using a microtiter plate assay based on the method of Bradford (30).

Two-dimensional gel electrophoresis of labeled proteins

For each gel (20 × 20 cm), 200 μg of protein was precipitated according to Wessel and Fluegge (31). The protein pellet was resolubilized in 340 μl of rehydration buffer [7 M urea, 2 M thiourea, 4% CHAPS, 0.002% (w/v) bromophenol blue, and 2% Pharmalyte™ 3–10] for 30 min at 37°C. Sample solutions were applied to 18 cm immobilized pH gradient strips (Immobiline DryStrip pH 3–10 NL; Amersham Biosciences) (32) by rehydration loading (33, 34). Isoelectric focusing and SDS-PAGE were performed as described previously (35, 36) using 10% polyacrylamide gels. After isoelectric focusing, Immobiline Dry Strip pH 3–10 NL strips were stored at −70°C. Gels were run in a PROTEAN® II XI Multi-cell 2-D apparatus (Bio-Rad) at 10°C, maintaining a limiting current of 50 mA/gel. After electrophoresis, gels were fixed in fixing solution (10% EtOH, 7% AcOH) for at least 2 h. Proteins were detected with the Molecular Imager® FX Pro Plus scanner (at a resolution of 100 μm) driven by PDQuest version 7.1.0 software (both from Bio-Rad). BODIPY fluorescence was determined using an external laser (Bio-Rad) at 488 nm for excitation and a 530/30 nm band-pass filter for the detection of emission. Total protein patterns were visualized by SYPRO Ruby Protein Gel Stain (Molecular Probes) according to the manufacturer's protocol. Scanning parameters for the SYPRO Ruby detection were the same as described previously, except that a 605 DF50 filter was used as the emission filter.

Stability of BODIPY-labeled phospholipids in cells

Confluent monolayer cultures of A7r5 cells in 100 mm Petri dishes were treated with the BODIPY analogs of PGPC (0.1 μM), POVPC (0.5 μM), or POPC (0.1 μM) in 10 ml of serum-free culture medium at 37°C for 5, 15, 30, 45, and 60 min. After incubation, cells were washed once with 10 ml of ice-cold PBS, scraped into 6 ml of ice-cold PBS with a rubber policeman (Corning), and then transferred into a pyrex tube. The culture dish was rinsed with an additional 3 ml of ice-cold PBS. The combined cell suspensions were centrifuged at 300 *g* and 4°C for 3 min. After discarding the supernatant, cellular lipids were extracted by a simplified procedure of Folch, Lees, and Sloane Stanley (37). The cell pellet was resuspended in 3 ml of $CHCl_3$/MeOH (2:1, v/v) and was shaken vigorously for 1 h at 4°C. After washing with 700 μl of a $MgCl_2$ solution (0.036% in water) and centrifuging at 80 *g* for 2 min at room temperature, the lower chloroform phase was collected and evaporated to dryness. In the case of BODIPY-POVPE, extracted lipids were reduced with 10 μM $NaCNBH_3$ in a biphasic system (a mixture of 1 ml of diethylether and 1 ml of buffer containing 0.75 M NaCl and 1 mM HEPES) (38), leading to the conversion of formed Schiff base adducts to stable amine structures. The reduced lipids were extracted from the aqueous phase with 5 ml of $CHCl_3$/MeOH (2:1, v/v). Finally, the isolated lipid mixtures were subjected to TLC (silica gel 60; Merck) using $CHCl_3$/MeOH/water (65:25:4, v/v/v) as a developing solvent. BODIPY-PGPE, -POVPE, and -POPE served as references (R_f = 0.27, 0.32, and 0.59, respectively). Fluorescence intensities of single spots were determined with a charge-coupled device camera (Herolab, Vienna, Austria) at an excitation wavelength of 365 nm using EasyWin® software for data acquisition.

Two-dimensional TLC separation of labeled cellular lipid extracts

A7r5 cells at high confluence in 100 mm Petri dishes were treated with 1 μM BODIPY-POVPE in 10 ml of serum-free culture medium for 30 min at 37°C. Lipid extraction was performed as described above. Reduction of the imines to secondary amines was carried out according to Friedman et al. (39) in the presence of 10 μM $NaCNBH_3$. Isolated lipids corresponding to 3–6 μg of phosphorus were applied onto a TLC plate (silica gel 60; Merck) (10 × 10 cm) and subjected to 2-D TLC separation using $CHCl_3$/MeOH/25% NH_3 (65:25:5, v/v/v) and $CHCl_3$/acetone/MeOH/glacial AcOH/water (50:20:10:10:5, v/v/v/v/v) as solvents in the first and second directions, respectively. Separated lipids were visualized by iodine vapor after the detection of fluorescent spots with a charge-coupled device camera as mentioned above.

Determination of acid sphingomyelinase activity

Rat aortic smooth muscle cells (A7r5) were grown on six-well plates until 80% confluency was reached. Growth was arrested with DMEM + 0.1% FCS for 24 h, and cells were subsequently incubated with BODIPY-PGPE, BODIPY-POVPE, POVPC, or

Downloaded from www.jlr.org by guest, on June 14, 2012

PGPC (10 μM each) for 30 min. After treatment of the smooth muscle cells with the respective compounds, cells were washed with cold PBS, scraped, harvested, and lysed by incubation with acid lysis buffer for the determination of acid sphingomyelinase activity using a fluorescent sphingomyelin substrate as described previously (26). Aliquots of cell lysates containing 1 μg of protein were analyzed for enzyme activity.

RESULTS

Synthesis and characterization of fluorescent PGPC and POVPC analogs

Chemical synthesis of seven fluorescently labeled phospholipids carrying a covalently bound BODIPY, Alexa647, or pyrene fluorophore was accomplished to study their interactions with VSMCs. The BODIPY- and Alexa647-labeled PGPC derivatives were prepared from PGPC by PLD-catalyzed head group exchange followed by *N*-acylation using BODIPY-SE (Fig. 1A) and Alexa647-SE, respectively. Esterification of 1-palmitoyl-*sn*-glycero-3-phosphocholine with 5,5-dimethoxypentanoic acid, subsequent exchange of choline against ethanolamine, covalent attachment of a BODIPY label to the head group, and final deprotection of the aldehyde group yielded BODIPY-POVPE (Fig. 1B). Synthesis of BODIPY-POPE was accomplished by the acylation of POPE with BODIPY-SE. Pyrene analogs of PGPC, POVPC, and POPC were obtained starting from 1,2-bis(10-pyrenedecanoyl)-*sn*-glycero-3-phosphocholine, which was converted to the corresponding 2-lysophospholipid by PLA_2. Acylation of this compound with glutaric anhydride or oleic acid completed the synthesis of PyrGPC (Fig. 1C) or PyrOPC, respectively. Condensation of 1-(10-pyrenedecanoyl)-*sn*-glycero-3-phosphocholine with 5,5-dimethoxypentanoic acid delivered a stable precursor of PyrOVPC, which was deprotected by carefully controlled hydrolysis (Fig. 1C). For more details, see Experimental Procedures.

The new BODIPY and pyrene derivatives were characterized by MALDI-TOF, as shown in **Fig. 2** and **Table 2**. In all cases, the expected molecular and pseudomolecular ions, respectively, were found. Simple replacement of cations gives the interpretation for the additional signals of (pseudo)molecular ions that are listed in Table 2.

The spectra of the BODIPY derivatives systematically showed additional intense signals. For example, the peak at *m/z* 806.41 Da in the spectrum of BODIPY-POVPE (Fig. 2A) can be interpreted as a monofluoro diazaborinium cation (40) formed from BODIPY-POVPE, protonated at the phosphate, via elimination of one fluoride ($[C_{40}H_{63}BFN_3O_{10}P]^+$, calculated *m/z* 806.43). H/Na exchange would give an ion $[C_{40}H_{62}BFN_3NaO_{10}P]^+$ that has a calculated mass of 828.42 Da, which corresponds well to the intense signal at 828.40 Da (Fig. 2A). Note that signals that could be assigned to corresponding diazaborinium cations were also observed in the mass spectra of BODIPY-PGPE and -POPE, indicating undesired side reactions during synthesis. Thus, commercially available BODIPY-SE, which was used during synthesis, was also investigated by MALDI-TOF MS. In addition to the expected pseudomolecular ion $[M{\cdot}Na]^+$, the spectrum clearly showed an intense signal that could be assigned to the corresponding monofluoro diazaborinium cation. Elimination of BF_2 was also detected in the MALDI spectrum of BODIPY-SE. These results imply that all additional intense signals that were observed in the MALDI spectra of the synthesized BODIPY phospholipids are cations formed during the MALDI process and that no undesired side reaction occurred during synthesis.

Fluorescence spectroscopic characterization of the labeled phospholipids yielded an excitation maximum of 505 nm and maximal emission at 510 nm for all BODIPY-labeled samples independent of the molecular species. As further summarized in Table 1, phospholipids carrying a pyrene fluorophore uniformly showed excitation and emission maxima at 342 and 376 nm, respectively. Thus, it can be concluded that coupling of either marker to the desired compounds did not significantly affect their spectral properties.

Similar structural tendencies become apparent when tentative space-filling models of POVPC and its pyrene and BODIPY analogs are compared (**Fig. 3**). The compounds shown have in common a large head group including the polar *sn*-2 substituent and only a single hydrophobic chain.

Import and intracellular distribution of fluorescent PGPC and POVPC analogs

For studies of the import of pyrene-, Alexa647-, or BODIPY-labeled phospholipids into VSMCs, serum-free medium was used to avoid degradation by lipolytic enzymes. Reference experiments showed that BODIPY-labeled analogs of PGPC and POVPC were hydrolyzed in the presence of 10% FCS within 2 h (data not shown). Moreover, cells showed no cytotoxic responses in terms of cell permeabilization and YO-PRO-1 penetrability (41, 42) in the specified time and concentration range of the fluorescent oxidized phospholipids, exemplified by 0.1 μM BODIPY-PGPE after an incubation period of 60 min.

In this study, we used BODIPY- and pyrene-labeled lipid analogs for the investigation of lipid import into the cells to detect potential effects of the fluorophore. Some differences were found between the fluorescence images of the PGPC analogs (15 min incubation) and the POVPC analogs at all incubation times. In this context, it has to be emphasized that pyrene fluorescence is much weaker and, in addition, is blue-shifted relative to the emission of BODIPY. As a consequence, the pyrene images are distorted by background fluorescence to a much larger extent. For the same reasons, the tiny contours of plasma membrane fluorescence are seen only with BODIPY but not with pyrene.

Significant intracellular accumulation of blue fluorescence in the perinuclear region was observed after incubation with PyrGPC (**Fig. 4A**) relative to untreated control cells (Fig. 4D), even after a period as short as 5 min. This effect persisted for the whole duration of treatment, leading to a steady increment of fluorescence intensity in this intracellular location. A slight staining of the plasma membrane became apparent after 15–30 min but was not

Downloaded from www.jlr.org by guest, on June 14, 2012

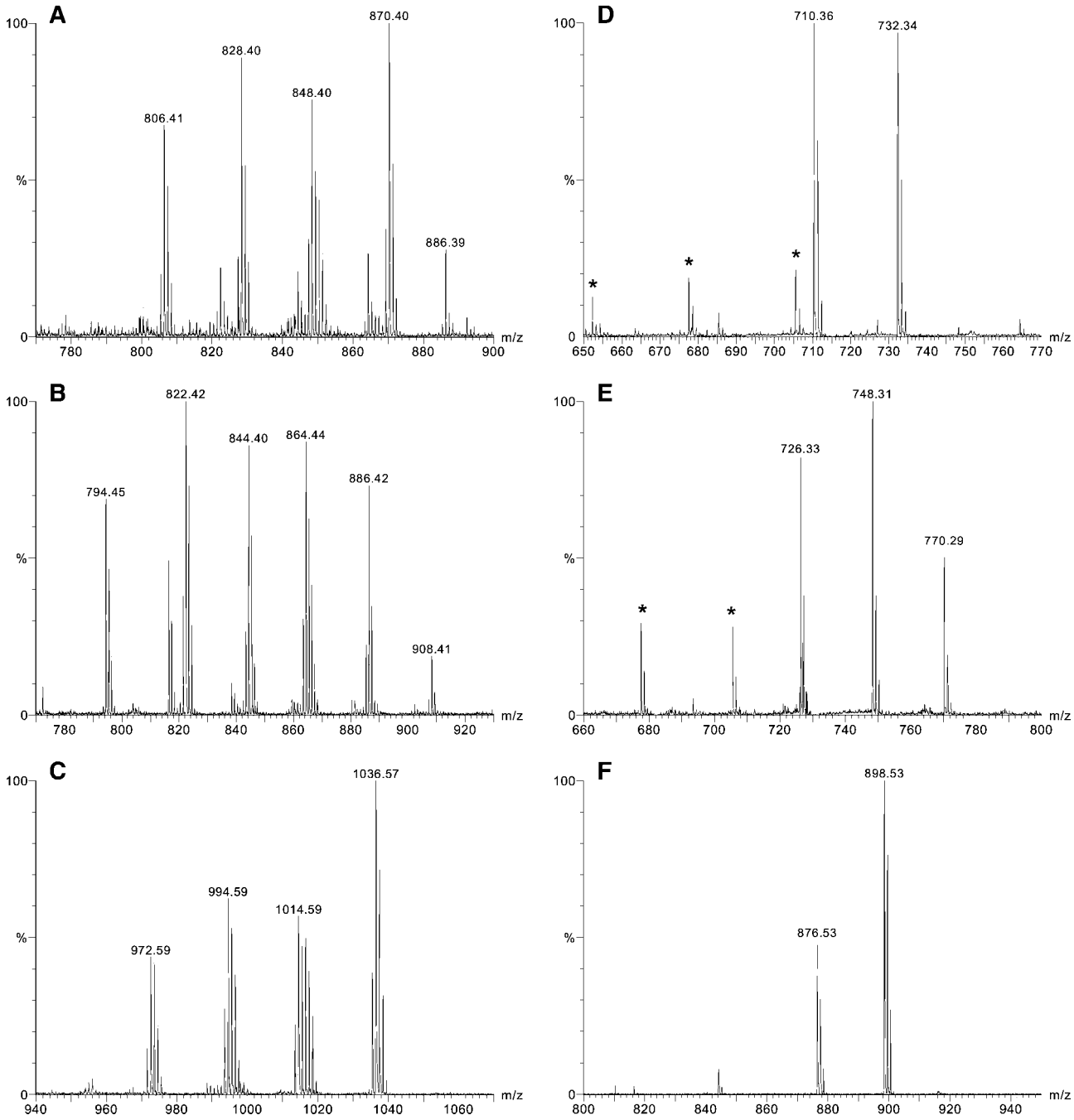

Fig. 2. Matrix-assisted laser desorption/ionization time-of-flight (MALDI-TOF) mass spectra of the synthesized BODIPY and pyrene derivatives. The graphs show expanded views of the important parts of the MALDI-TOF mass spectra. Compare Table 2 and see text for discussion. Matrix cluster ions are marked with asterisks. A: BODIPY-POVPE. B: BODIPY-PGPE. C: BODIPY-1-palmitoyl-2-oleoyl-*sn*-glycero-3-phosphoethanolamine (POPE). D: PyrOVPC. E: PyrGPC. F: 1-(10-Pyrenedecanoyl)-2-oleoyl-*sn*-glycero-3-phosphocholine (PyrOPC).

further intensified during longer incubation times. The staining pattern of PyrGPC was very similar to that seen when cells were treated with BODIPY-PGPE. At early time points, only regions in close proximity to the cell nucleus fluoresced brightly, whereas later, weak surface labeling occurred and increased in intensity. Under the same experimental conditions, Alexa647-PGPE partitioned in an analogous manner after 5 and 30 min.

There was an almost perfect overlay of the fluorescence patterns of BODIPY-PGPE and the blue emission of the LysoTracker (**Fig. 5A**), which is indicative of preferential lipid localization to the lysosomes. Colocalization studies with an ER-specific marker revealed that the endoplasmic reticulum hardly accumulated fluorescent PGPC analogs (Fig. 5B). No colocalization of a mitochondrion-selective probe with BODIPY-PGPE (Fig. 5C) was observed.

Transfer of BODIPY-POVPE was less efficient compared with BODIPY-PGPE, although the concentration was 5-fold higher in the case of the former lipid (Fig. 4B). After 5 min of treatment, mainly autofluorescence was

Downloaded from www.jlr.org by guest, on June 14, 2012

TABLE 2. Interpretation of signals observed in the matrix-assisted laser desorption/ionization time-of-flight mass spectra of the synthesized BODIPY and pyrene derivatives

Interpretation	1-Palmitoyl-2-(5-oxovaleroyl)-*sn*-glycero-3-phosphocholine	1-Palmitoyl-2-glutaroyl-*sn*-glycero-3-phosphocholine	POPC
BODIPY analogs			
$[(M-BF_2+H)\cdot H]^+$	778.45 (778.44)	794.45 (794.44)	944.61 (944.65)
$[(M-BF_2+H)\cdot Na]^+$	800.40 (800.42)	816.43 (816.42)	966.54 (966.63)
$[(M-BF_2+Na)\cdot Na]^+$	822.39 (822.40)	838.40 (838.40)	988.57 (988.61)
$[M-F]^+$	806.41 (806.43)	822.42 (822.43)	972.59 (972.64)
$[(M-H+Na)\text{-}F]^+$	828.40 (828.42)	844.40 (844.41)	994.59 (994.62)
$[(M-H+K)\text{-}F]^+$	844.40 (844.39)		
$[M\cdot Na]^+$	848.40 (848.42)	864.44 (864.42)	1,014.59 (1,014.63)
$[M\cdot K]^+$	864.38 (864.40)		
$[(M-H+Na)\cdot Na]^+$	870.40 (870.40)	886.42 (886.40)	1,036.57 (1,036.61)
$[(M-H+Na)\cdot K]^+$	886.39 (886.38)		
$[(M-2H+2Na)\cdot Na]^+$		908.41 (908.38)	
Pyrene analogs			
$[M]^+$	710.36 (710.35)	726.33 (726.34)	876.53 (876.55)
$[M-H+Na]^+$	732.34 (732.33)	748.31 (748.32)	898.53 (898.54)
$[M-2H+2Na]^+$		770.29 (770.30)	
$[2M-H]^+$	1,419.69 (1,419.68)	1,451.62 (1,451.67)	1,752.21 (1,752.10)
$[2M-2H+Na]^+$	1,441.69 (1,441.67)	1,473.59 (1,473.66)	1,774.15 (1,774.08)
$[2M-3H+2Na]^+$		1,495.60 (1,495.64)	

Comparison of measured and calculated *m/z* values (calculated values are shown in parentheses; all calculated values correspond to the most intense peak of any isotope distribution). M is generally used as an abbreviation for species with P-OH and -COOH groups (neutral species in the case of the BODIPY derivatives, cation NR_4^+ for pyrene derivatives). Compare Fig. 2 and see text for discussion.

detectable (Fig. 4D). During prolonged incubations (15–90 min), high BODIPY fluorescence was seen in the plasma membrane of VSMCs. At this stage, the label highlighted plasma membrane domains and budding vesicles at the surface along the cell outline, probably constituting the forerunners of released membrane bodies (43). The fluorescence of BODIPY-POVPE overlapped extensively with the FM 1-43 membrane probe, which is believed to insert into the outer leaflet of the plasma membrane (Fig. 5D). No colocalization of a mitochondrion-selective probe with BODIPY-POVPE (data not shown) was observed.

PyrOVPC basically showed the same fluorescence pattern as its BODIPY analog. However, the plasma membrane staining after long incubation times was less pronounced. This is very likely attributable to the fact that pyrene at sufficiently high concentrations in the bilayer may form excited-state dimers (excimers) upon excitation emitting at ~470 nm, although with a lower intensity compared with the blue monomer (44).

Fluorescent POPC analogs (pyrene- or BODIPY-labeled) as nonoxidized reference compounds with two long hydrophobic chains were not efficiently taken up by the cells in the same time domain and, in addition, showed a different intracellular distribution pattern (Fig. 4C). In summary, it is quite obvious that short-chain oxidized phospholipids partition into cells very fast and are targeted to different subcellular compartments compared with the more hydrophobic double-chain phospholipids.

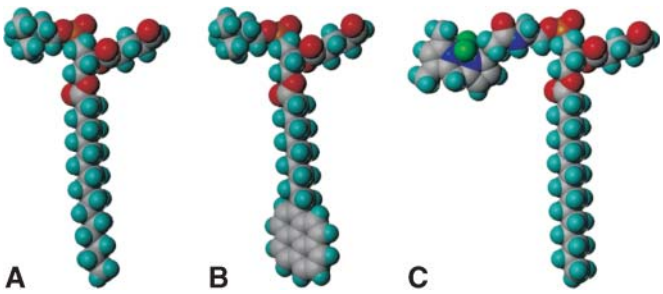

Fig. 3. POVPC and its fluorescent analogs share essential structural features. Tentative space-filling models of POVPC (A), PyrOVPC (B), and BODIPY-POVPE (C) are shown (SYBYL software). Note the high similarity of the natural lipid and its derivatives, especially the pyrene analog, all of them sharing a single long hydrophobic chain and a large polar head group.

Uptake of pyrene-labeled POVPC analogs depends on LDL internalization

In addition to pure dispersions of oxidized phospholipids, we used LDL as a delivery system for the import of these compounds into cells. When A7r5 cultures were incubated with LDL (50 μg protein/ml) containing PyrGPC (3 nmol/μg protein), a significant amount of the labeled lipid was already transferred to cells after 15 min (**Fig. 6A**). The pattern of intracellular fluorescence was similar to that observed previously using pure PyrGPC dispersions (Fig. 4A). Longer incubations (45 min) led to an additional accumulation of blue fluorescence in internal structures around the nucleus, with only a tiny fraction being located in the plasma membrane. In contrast, different images were obtained when cells were treated with LDL (50 μg protein/ml) preloaded with PyrOVPC (5 nmol/μg protein) compared with pure lipid aggregates as donor systems. Surface labeling still occurred, but the amount of internalized lipid was much higher and the distribution pattern was different (Fig. 6B). Obviously, the

Downloaded from www.jlr.org by guest, on June 14, 2012

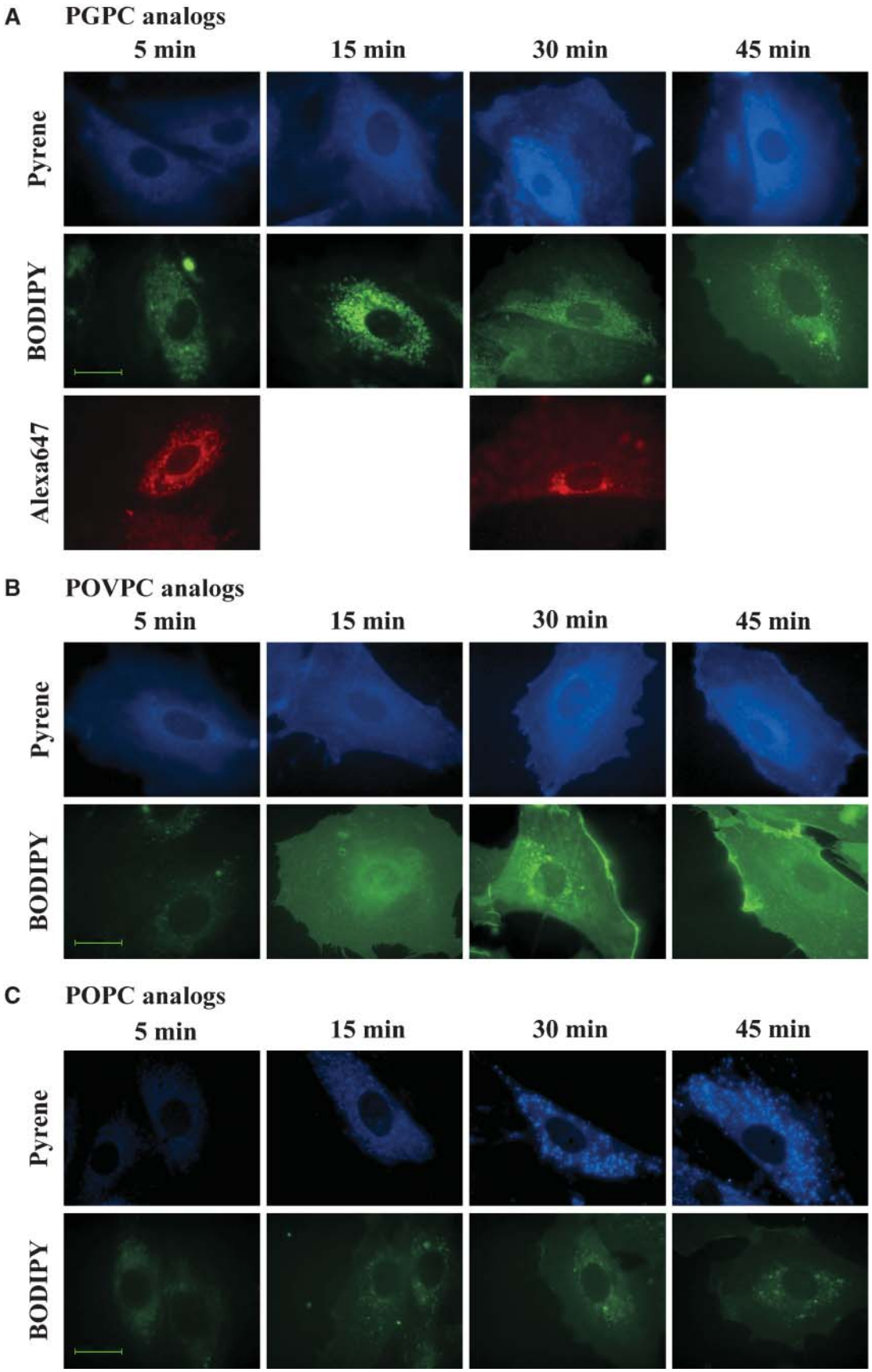

Fig. 4. Continued.

Downloaded from www.jlr.org by guest, on June 14, 2012

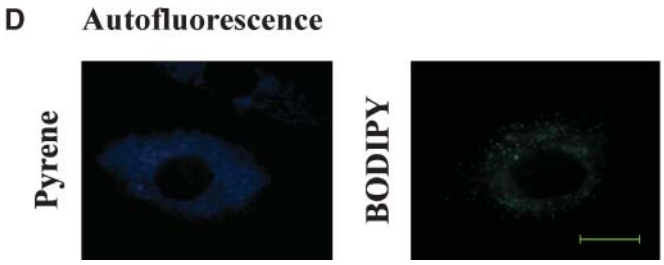

Fig. 4. Time-dependent uptake of fluorescent PGPC, POVPC, and POPC analogs into vascular smooth muscle cells (VSMCs). A–C: A7r5 cells were incubated with 0.1 μM BODIPY-PGPE, 2 μM PyrGPC, or 0.1 μM Alexa647-PGPE (A), 0.5 μM BODIPY-POVPE or 2 μM PyrOVPC (B), and 0.1 μM BODIPY-POPE or 2 μM PyrOPC (C) in serum-free culture medium for 5, 15, 30, or 45 min at 37°C, washed twice with PBS, and observed by fluorescence microscopy. D: Autofluorescence micrographs of VSMCs treated with culture medium without fetal calf serum (FCS) for 5–60 min. No differences could be observed for varying incubation periods. Using the optical settings for Alexa647, absolutely no background was detected. Photomicrographs shown are representative of at least five cells for each time point in three or more independent experiments, with the exception of the Alexa647 images (single experiment). For a given microscope channel, all photomicrographs were exposed and printed identically. Bars = 20 μm. Fluorescent derivatives of both oxidized phospholipids are rapidly internalized by VSMCs, in contrast to their POPC equivalents. Note the remarkable differences in their intracellular distribution. PGPC analogs are initially transferred to perinuclear regions, whereas in POVPC derivatives, fluorescence becomes highly enriched in the plasma membrane during short incubation times. There is a high correlation between photomicrographs obtained from each phospholipid species independent of the type and the binding site of the respective label.

LDL particles change the (unknown) mechanism of translocation and distribution of the fluorescent POVPC analog in VSMCs.

In a further attempt to specify the role of LDL in delivering oxidized phospholipids to vascular wall cells, we conducted dual-color experiments with LDL labeled with BODIPY at apolipoprotein B-100 (apoB) and traces of fluorescent (pyrene-labeled) PGPC and POVPC in the lipid phase (Fig. 6C, D). Import rates and intracellular targeting of the fluorescent phospholipids seem unchanged compared with LDL, in which only the lipid was labeled. In this context, it is important to emphasize that only lipid (pyrene) fluorescence but no LDL (BODIPY) emission could be detected intracellularly. The cells we used in these experiments were not fasted and thus show very low expression of the LDL receptor. By this means, it was possible to selectively study the import of the lipid component into the cells, which appears to be different for the fluorescent PGPC and POVPC analogs.

Stability of BODIPY-labeled PGPC and POVPC analogs in cells

Lipid extraction of cells after incubation with BODIPY-PGPE followed by TLC analysis showed limited stability of this compound in VSMCs. A new fluorescent lipid was formed corresponding to the respective lysophospholipid on TLC (**Fig. 7**). Experiments to determine the stability of the pyrene-labeled PGPE under reasonable conditions relevant to the fluorescence microscopy studies (0.1 mM lipid concentration) failed. Pyrene fluorescence is lower than BODIPY fluorescence by at least 1 order of magnitude and, in addition, blue-shifted. Thus, it is not detectable in the background fluorescence of the lipid extract. According to all we know from lipids labeled with pyrene in the acyl chain (minimum perturbing effect) (45), these compounds are better substrates for enzymes. Therefore, pyrene-PGPE is likely to be hydrolyzed faster inside the cells compared with the BODIPY derivative.

BODIPY-POVPE exhibited a more complex behavior. 2-D TLC analysis revealed a number of new products (**Fig. 8**) that have not been identified yet and are currently subject to identification by mass spectrometry. Comparison of the TLC separation of the modified lipids with extracts obtained from reactions of BODIPY-POVPE with phosphatidylethanolamine and phosphatidylserine (data not shown) shows identical fluorescence patterns (indicated by arrows in Fig. 8A, B). From the literature, it is known that the aldehydolipids might undergo aldol condensation with themselves (39) and form (Schiff base) adducts with endogenous cellular lipids (phosphatidylethanolamine and phosphatidylserine) (38, 46).

In addition, BODIPY-POVPE showed reactivity toward proteins. 2-D gel electrophoresis of total protein extracts from cells pretreated with BODIPY-POVPE (2.5 μM, 30 min) demonstrated several fluorescent spots corresponding to covalent adducts of the oxidized lipid with cellular polypeptides (**Fig. 9**). They represent primary molecular targets of aldehyde-containing phospholipids and are currently subject to identification by nano-HPLC-MS/MS.

To address the question of whether the cellular distribution of the fluorescent lipid analogs represents the behavior of their unlabeled counterparts, at least in a qualitative manner, we determined their effect on the activation of acid sphingomyelinase, which is a key component of the apoptotic signaling induced by PGPC and POVPC (11). The data presented in **Fig. 10** show that both PGPC and POVPC as well as the respective fluorescent analogs BODIPY-PGPE and BODIPY-POVPE activate the enzyme in VSMCs.

DISCUSSION

In this article, we describe the uptake, distribution, and modification of different fluorescently labeled derivatives of PGPC, POVPC, and POPC in VSMCs. The incubations were performed in serum-free medium to demonstrate how the intact fluorescent phospholipids are taken up into cells without interference with the serum components. Because the biological relevance of such a study depends on the interaction of the labeled compounds with the lipids and proteins in serum, we determined the stability of PGPC and POVPC in 10% FCS (46a). Both phospholipids were found to be entirely hydrolyzed in FCS within several hours. After 1 h, ~50% of the lipids were degraded. Therefore, we would have seen a mixture

Downloaded from www.jlr.org by guest, on June 14, 2012

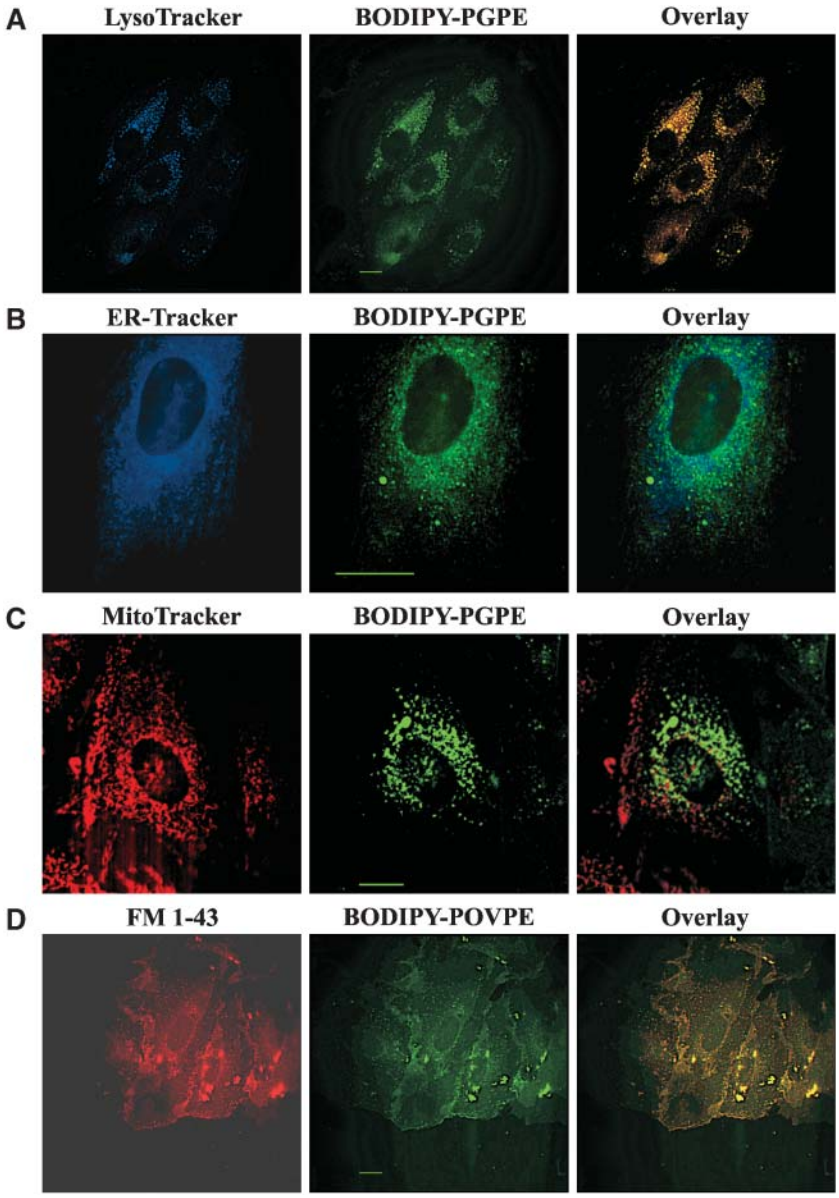

Fig. 5. Colocalization of BODIPY-PGPE and BODIPY-POVPE with organelle-specific markers in VSMCs. Subcellular distribution of BODIPY-PGPE in VSMCs with respect to various organelle-specific markers. A–C: A7r5 cells were pretreated with LysoTracker Blue DND-22 (160 nM) (A), ER-Tracker Blue-White DPX (200 nM) (B), or MitoTracker Red CMXRos (200 nM) (C) for 30 min, followed by incubation with 10 nM BODIPY-PGPE in supplemented DMEM without serum for 15 min. Fluorescence images of both the BODIPY phospholipid and the organelle-specific probes were recorded from the same field of cells and then used to produce overlays of the double staining. Note the extensive colocalization of BODIPY and LysoTracker fluorescence. Although partial delivery of the labeled lipid to the endoplasmic reticulum (ER) is also evident, mitochondria can be excluded as an intracellular destination of exogenously supplied BODIPY-PGPE under the experimental conditions used. D: Treatment of A7r5 cells with BODIPY-POVPE in serum-free culture medium for 15 min and image acquisition preceded incubation with FM 1-43 membrane probe (150 nM) in fresh medium without FCS for 30 min. The field previously imaged for BODIPY fluorescence was rephotographed for FM 1-43 fluorescence. The extensive overlap of the dual-labeled structures suggests a predominant accumulation of BODIPY-POVPE in the plasma membrane of VSMCs. Photomicrographs shown are representative of at least three independent experiments. In control experiments, hardly any crossover between green (BODIPY-PGPE), blue (LysoTracker, ER-Tracker), and red (MitoTracker, FM 1-43) fluorescence channels was detected at these concentrations. For a given microscope channel, all photomicrographs were exposed and printed identically. Bars = 20 μm.

Downloaded from www.jlr.org by guest, on June 14, 2012

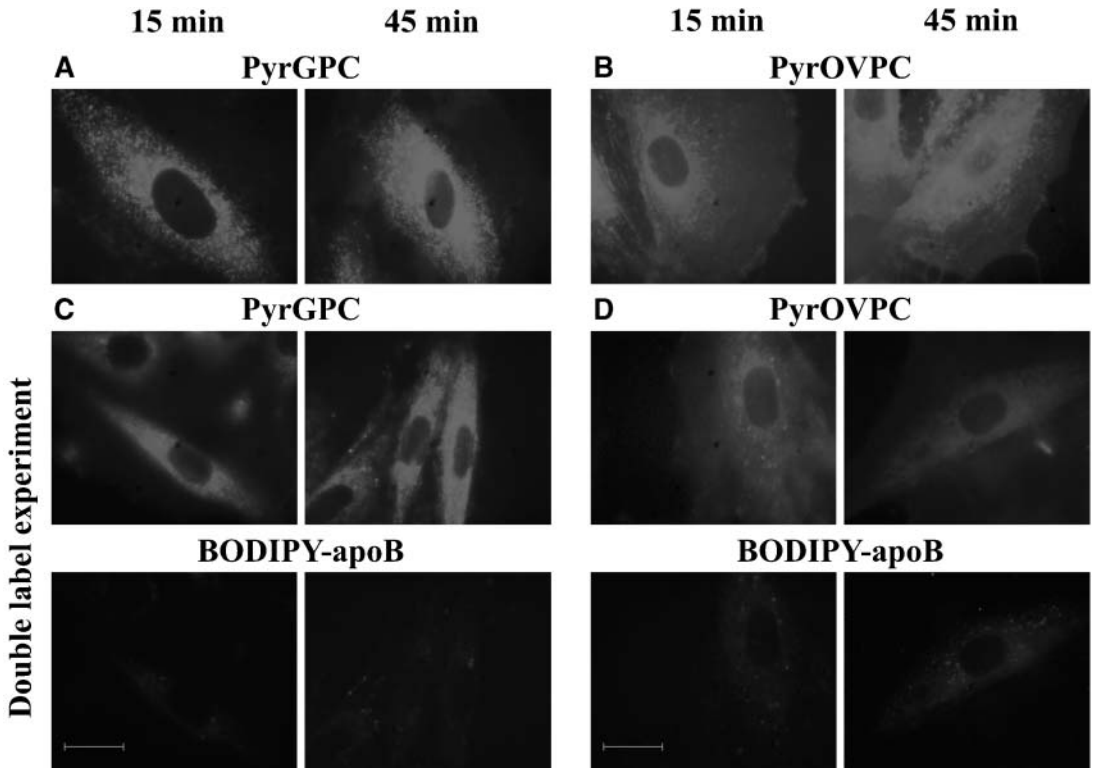

Fig. 6. Transfer of PyrGPC and PyrOVPC from LDL into VSMCs. A7r5 cells were incubated with LDL/PyrGPC (50 μg protein/ml; 3 nmol PyrGPC/μg protein) (A), LDL/PyrOVPC (50 μg protein/ml; 5 nmol PyrOVPC/μg protein) (B), BODIPY-LDL/PyrGPC (50 μg protein/ml; 3 nmol PyrGPC/μg protein) (C), and BODIPY-LDL/PyrOVPC (50 μg protein/ml; 5 nmol PyrOVPC/μg protein) (D) in serum-free culture medium for 15 or 45 min at 37°C, washed twice with PBS, and observed with the fluorescence microscope. Images were acquired at blue (pyrene) and green (BODIPY) wavelengths. Photomicrographs shown are representative of at least three cells for each time point in three independent experiments. In control experiments, hardly any crossover between green (BODIPY) and blue (pyrene) wavelengths was detected at these concentrations. For a given microscope channel, all photomicrographs were exposed and printed identically. Bars = 20 μm. Similar uptake rates and fluorescence patterns were observed for PyrGPC and PyrOVPC when delivered from single (A, B) or double (C, D) labeled LDL, indicating no interference of the attached BODIPY fluorophore with the phospholipid exchange process. Note that the intracellular fluorescence pattern obtained after treatment with LDL, which was prelabeled with pyrene analogs of either oxidized phospholipid, highly resembles the distribution observed when cells were incubated with aqueous dispersions of fluorescent PGPC derivatives (see Fig. 4A, B). The absence of green intracellular labeling (C, D) indicates no uptake of LDL by VSMCs under these experimental conditions. apoB, apolipoprotein B-100.

of the intact labels as well as their hydrolysis products, especially at the long incubation times, if we had measured lipid transport into cells under high-serum conditions. However, uptake of the labeled lipids into the cells is fast and becomes detectable within minutes. Recent millisecond-resolved fluorescence microscopy studies on the single-molecule level support this assumption. These high-resolution experiments showed that the oxidized PL is already taken up into the plasma membrane within seconds, followed by very fast clustering and endocytosis by plasma membrane vesicles (Sebastian Rhode, PhD thesis, 2006, University of Linz, Austria). Interestingly, the specific biological response (activation of acid sphingomyelinase and mitogen-activated protein kinases) (11) also occurs within a few minutes after addition of the oxidized lipids to the cells under conditions in which extracellular and intracellular hydrolysis of the oxidized phospholipid is only minimal. Nevertheless, a systematic study will be necessary to investigate the quantitative and long-term effects of serum and its individual components [e.g., albumin, lipoproteins (Fig. 6), lipolytic enzymes] that are relevant to the extracellular stability and transport of the oxidized phospholipids into cells. Such work is currently under way in our laboratory.

To exclude or better estimate the influence of the lipid-bound fluorophore, we synthesized up to three differently labeled analogs to verify the relevance of our observations. In these approaches, we set a high value on conforming size and polarity of the marker to match the properties of the unlabeled parent compounds as closely as possible. The BODIPY fluorophore was chosen by virtue of its high fluorescence yield and great photostability. Because of its rather polar nature, it was linked to the head group of the phospholipid molecules. The same applies to the even more polar Alexa647 label, which has proven to be particularly suitable for minimizing background fluorescence. In contrast, the spectral properties of pyrene analogs do not allow for high-sensitivity detection, but they have the advantage of carrying a hydrophobic label at the ω terminus of the long *sn*-1 acyl chain. If embedded

Downloaded from www.jlr.org by guest, on June 14, 2012

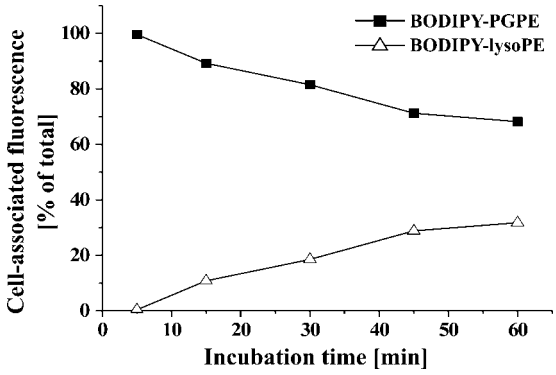

Fig. 7. Degradation of BODIPY-PGPE in VSMCs. A7r5 cells were incubated for the indicated times with 0.1 μM BODIPY-PGPE in serum-free medium, washed, and collected. After lipid extraction and TLC separation, BODIPY fluorescence was quantified directly on the TLC plates. BODIPY-PGPE was continuously hydrolyzed to BODIPY-phosphoethanolamine (lysoPE), which constitutes the only newly formed fluorescent spot. Data are representative of two independent experiments producing similar results.

in a membrane, the marker will most likely reside in the very center of the bilayer, where the molecular order and, thus, membrane perturbation should be minimal (45).

Our fluorescence microscopy experiments indicate high agreement between data obtained from the same phospholipid species containing different labels. Thus, it may be concluded that the observed phenomena can be attributed to innate properties of the lipid molecules rather than to the attached fluorophores. This is not surprising, because the fluorescent derivatives and their parent compounds share basic structural features. As tentatively illustrated in Fig. 3, they are characterized by a single hydrophobic chain and an oversized polar head group, both of which in combination confer high surface activity. Taking this into consideration, it can be expected that oxidized phospholipids are rapidly exchanged between membranes and/or liposomes. Previous studies have demonstrated that, when cells or lipid vesicles are incubated with liposomes containing another short-chain phospholipid, 1-acyl-2-(*N*-4-nitrobenzo-2-oxa-1,3-diazole)-aminocaproyl phosphatidylcholine, the fluorescent lipid spontaneously transfers between membranes (47). The mechanism for this transfer has been demonstrated to be diffusion of soluble fluorescent lipid monomers (48). It is very likely that the exchange of the even more polar oxidized phospholipids under investigation between the donor particles and cells is driven by the same process. Moreover, the oxidized phospholipids are probably monomeric, as lysolecithin, whose polarity resembles that of oxidized phospholipids, has a critical micelle concentration of 450 ± 60 μM in aqueous solution at 25°C (49), far higher than the concentration of the oxidized lipids under the incubation conditions used (0.1–2 μM).

Indeed, fluorescence microscopy revealed very fast uptake of synthetic PGPC analogs by VSMCs, resulting in a lysosomal distribution pattern (Fig. 5A). It was not

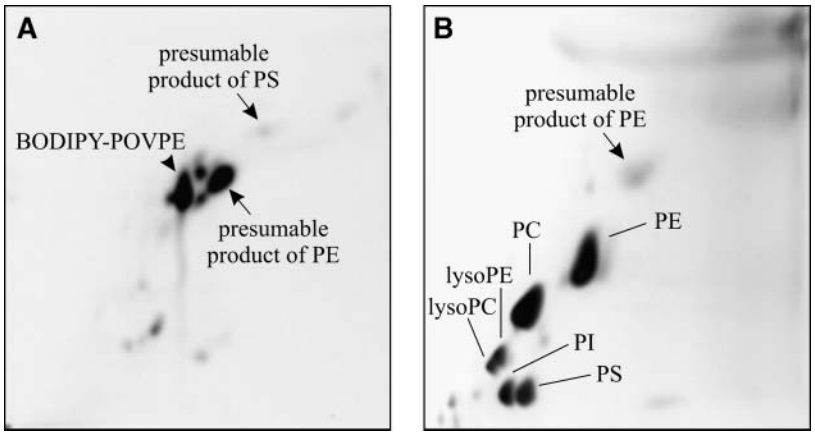

Fig. 8. Detection of modified lipids in VSMCs by covalent labeling with BODIPY-POVPE. Total lipid extracts from A7r5 cells were preincubated with 1 μM BODIPY-POVPE in serum-free culture medium (see Experimental Procedures). After reduction with 10 μm $NaCNBH_3$, they were separated by two-dimensional (2-D) TLC using $CHCl_3$/MeOH/25% NH_3 (65:25:5, v/v/v) and $CHCl_3$/acetone/MeOH/glacial AcOH/water (50:20:10:10:5, v/v/v/v/v) in the first and second direction, respectively. The starting point was the lower left corner. A: Lipid products with the fluorescent phospholipid were detected with a charge-coupled device camera as described in Experimental Procedures. Arrows indicate fluorescent spots most likely corresponding to modified cellular lipids, presumably phosphatidylethanolamine (PE) and phosphatidylserine (PS). The arrowhead denotes intact BODIPY-POVPE. The remaining fluorescent spots probably represent self-condensation products of the same compound. B: Iodine vapor was used as a general lipid stain. However, unsaturated lipids are more intensely stained. This is probably the reason why most of the fluorescent spots apart from the presumed phosphatidylethanolamine product could hardly be visualized by this method, as they consist mainly of BODIPY-POVPE containing only a single saturated fatty acyl chain. PC, phosphatidylcholine; PE, phosphatidylethanolamine; PI, phosphatidylinositol; PS, phosphatidylserine.

Downloaded from www.jlr.org by guest, on June 14, 2012

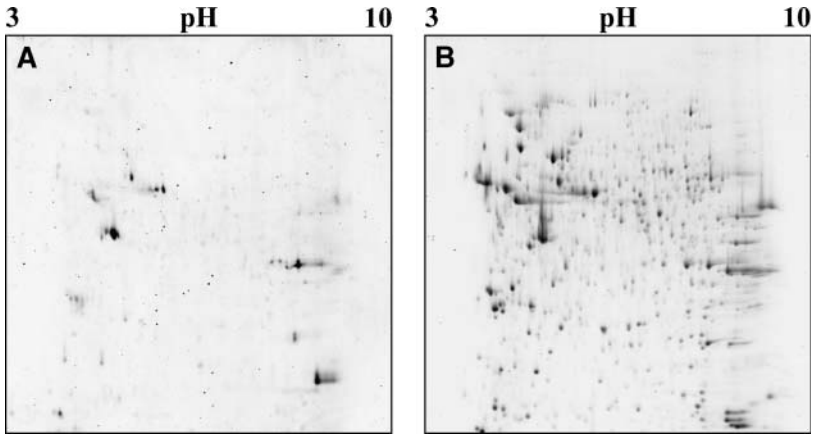

Fig. 9. Detection of primary protein targets in VSMCs by covalent labeling with BODIPY-POVPE. Total protein extracts from A7r5 cells preincubated with 2.5 μM BODIPY-POVPE in PBS (see Experimental Procedures) were separated by 2-D gel electrophoresis after reduction with 70 μM $NaCNBH_3$. A: Protein adducts with the fluorescent phospholipid were detected with a laser scanner as described in Experimental Procedures. B: SYPRO Ruby Protein Gel Stain was used to visualize total protein. Note that not all but still numerous proteins, including low-abundance proteins, became visible under the experimental conditions used, indicating covalent modification by BODIPY-POVPE.

until 30 min that a slight but distinctive staining of the plasma membrane became visible as well. The pathway by which intracellular membranes are labeled by PGPC derivatives is unknown. One possible explanation is that intact PGPC derivatives are targeted directly to the lysosomes, reflecting either vesicular movement or monomeric diffusion. Alternatively, staining of ER membranes may be the result of lipid degradation. The latter possibility could be ruled out by the finding that the half-time of BODIPY-PGPE in VSMCs is >1 h. Figure 7 shows the partial hydrolysis of BODIPY-PGPE to the respective lysolipid as the only fluorescent metabolite newly formed. This observation gives rise to the notion that the apoptotic signaling, which has been shown to be triggered by PGPC within 10 min (11), can be ascribed without much doubt to intact molecules of the oxidized phospholipid. Nevertheless, it cannot be excluded that the repartition of fluorescence during prolonged incubations originates from the anterograde translocation of cumulative hydrolytic degradation products.

The converse situation, in which prominent staining of the plasma membrane clearly precedes an intracellular increment of fluorescence intensity, was observed when cells were incubated with the aldehydolipid (POVPC) derivative for short periods of time (Fig. 4B), perhaps as a consequence of covalent reaction with amino and other groups in lipids and proteins. Previous reports already demonstrated that other aldehydes, particularly 4-hydroxy-2-nonenal (HNE), are able to react with amino groups of lysines and histidines and with sulfhydryl groups of proteins and peptides, leading to the formation of HNE adducts with cellular proteins during oxidative stress (50, 51). Of great relevance to this work is the fact that HNE can activate the epidermal growth factor receptor and its downstream signaling cascades merely through derivatization of reactive amino groups (52, 53). On the other

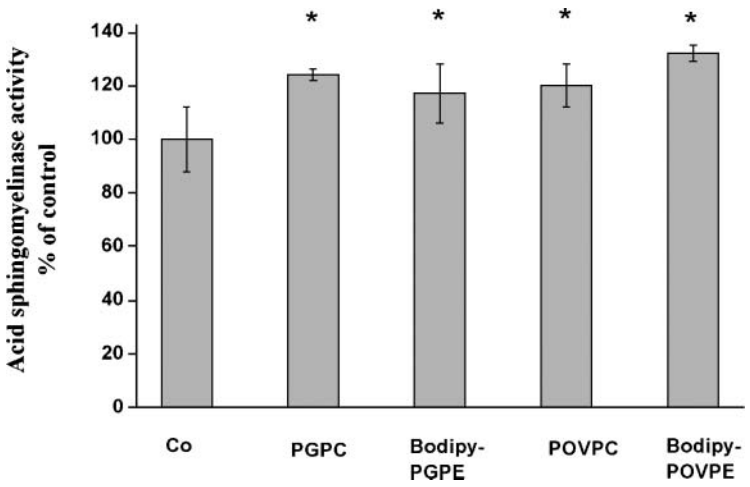

Fig. 10. Effects of BODIPY-labeled and unlabeled oxidized phospholipids on acid sphingomyelinase activity in VSMCs. Rat aortic smooth muscle cells (A7r5) were incubated with BODIPY-PGPE, BODIPY-POVPE, POVPC, or PGPC (10 μM each) for 30 min. Cells were isolated and lysed in lysis buffer for the determination of acid sphingomyelinase activity (see Experimental Procedures). Enzyme activities were measured as described previously (26) and expressed as percentage of control (Co). Data are means ± SD (n = 3). * $P < 0.05$ compared with control.

Downloaded from www.jlr.org by guest, on June 14, 2012

hand, aldehydes generated by the myeloperoxidase system of phagocytes were shown to covalently modify the amino groups of ethanolamine and serine glycerophospholipids to form biologically active Schiff base adducts (46). Zieseniss et al. (38) found that Schiff base adducts between phosphatidylethanolamine and aldehydes in oxidized LDL provoke the stimulation of platelet prothrombinase activity. In the beginning, there was little consideration of the possibility that some of the masking of amino groups during LDL oxidation might be attributable to conjugation with phospholipid aldehydes, as exemplified by POVPC. Several studies now exist that demonstrate covalent adduct formation between oxidized phospholipids and apoB (13, 38, 54). In this work, we found evidence that BODIPY-POVPE reacts with many cellular proteins. Multiple fluorescent protein spots could be detected upon separation of prelabeled cell protein extracts by 2-D gel electrophoresis (Fig. 9). In addition, 2-D TLC revealed that at least one fraction of cell lipid was also covalently modified by BODIPY-POVPE (Fig. 8). In summary, it seems possible that POVPC is inserted rapidly into the plasma membrane of VSMCs during its first contact with the cell surface, resides there in covalent association with amine-containing lipids and proteins, and is subsequently, at least in part, transferred in the form of Schiff bases to perinuclear regions.

Another interesting point pertaining to the current study is the finding that the way that oxidized phospholipids are presented to VSMCs has some influence on their uptake rates and intracellular distribution. LDL enriched with the pyrene analogs of PGPC yielded a fluorescence pattern similar to that observed when cells were treated with aqueous dispersions of the respective lipids. In contrast, the import of LDL-associated pyrene-POVPC was more efficient compared with that of the free lipid. Experiments with dual-labeled LDL (BODIPY at apoB, green fluorescence; pyrene-labeled lipids, blue fluorescence) produced the same results. All experiments were conducted with nonfasted cells, which means that LDL receptor expression at the cell surface was repressed (55). Thus, LDL internalization is only partially involved in the observed effects, and lipid import takes place via lipid transfer to a large extent. Obviously, the polar truncated phospholipids are easily exchangeable between different lipoprotein particles and/or cellular membranes. In this way, they can broaden their cross-section of action beyond a single cell or particle, thus exerting biological activity distant from their sites of origin. This idea is in agreement with the results of Podrez et al. (56), who suggested that oxidized phospholipids not adducted to apoB within oxidized LDL can transfer to native LDL and induce CD36 recognition by macrophages. By this means, they can be considered important mediators of cytotoxic effects (11) elicited by oxidative stress in other parts of biological systems as well. For instance, the possibility that oxidized phospholipids are transferable between oxidized LDL and intact HDL may lead to multiple functions in the development of atherosclerosis (57).

In contrast to POVPC, the cellular effects attributable to PGPC are entirely physical. Owing to its excellent membrane-perturbing capacity, it is conceivable that PGPC is capable of altering lipid packing, perhaps not only in fluid but also in more rigid microdomains such as rafts or caveolae (58). Many receptor-mediated signaling systems may be localized to and operate through caveolae, including epidermal growth factor receptor, Ras, and trimeric G-proteins, among others (59). Any membrane protein, but particularly ion channels, may be regulated via the cellular control of membrane composition, as indicated by the responsiveness of specific ion channels to changes in the lipid environment (60). Differences in the biophysical properties of membrane microdomains (e.g., fluidity) have been suggested to play a role in the sorting of proteins and lipids into different subpopulations of intracellular transport vesicles (61, 62), possibly resulting in abnormal trafficking. Thus, the physical interaction of PGPC with cellular components or the deregulation of key signaling pathways that probably operate through membrane microdomains could lead to aspects of the differentiated VSMC phenotype.

In general, the physical interaction and covalent modification of cellular components by oxidized phospholipids exhibit only poor specificity, which suggests the involvement of various mediators and the induction of a wide range of biological effects. PGPC and POVPC have been reported to elicit apoptotic signaling in VSMCs (11). Issues that remain to be clarified include the identification of their primary molecular targets. Here, we demonstrate the presence of multiple interaction sites for oxidized phospholipids on the cell surface as well as inside VSMCs. It is intriguing to consider the possibility that signal transduction pathways might be activated simultaneously at different levels, even bypassing early signaling elements.

Walton et al. (19, 63) suggested that the induction of interleukin-8 transcription by oxidized 1-palmitoyl-2-arachidonoyl-*sn*-glycero-3-phosphocholine is mediated by a 37 kDa glycosylphosphatidylinositol-anchored protein that interacts with Toll-like receptor 4. On the basis of studies in *Xenopus laevis* oocytes, Leitinger and colleagues (64) concluded that POVPC and PGPC elicit their cellular responses through binding to different receptors. This adds to earlier indications that the effects of oxidized phospholipids are receptor-mediated. Abolishment of their cellular responses by platelet-activating factor receptor antagonists implies a central role for this receptor in activating VSMCs, endothelial cells, monocytes, platelets, and neutrophils (10, 65–67). Subbanagounder et al. (68) have provided evidence that the in vitro effects of POVPC and 1-palmitoyl-2-(5,6-epoxyisoprostane E_2)-*sn*-glycero-3-phosphocholine, another bioactive lipid present in minimally modified LDL (69), probably are not mediated by the platelet-activating factor receptor. They do not exclude a role for it in the action of these two molecules and speculate that there might exist a separate WEB 2086-sensitive receptor for POVPC and 1-palmitoyl-2-(5,6-epoxyisoprostane E_2)-*sn*-glycero-3-phosphocholine. We acknowledge the involvement of membrane proteins in particular processes activated by oxidized phospholipids, but in the light of the data presented here, we doubt the

Downloaded from www.jlr.org by guest, on June 14, 2012

exclusive role of specific receptors for these compounds and support the notion that the majority of the observed effects result from many different interactions with components of their microenvironment. This idea is consistent with the results of Kogure et al. (23) suggesting that apoptosis induced by oxidized LDL-derived phospholipids in VSMCs is caused by temporary membrane distortion and not through specific receptors.

Further studies are needed to elucidate the mechanisms underlying the pathophysiological effects of oxidized phospholipids on VSMCs. The identification of their primary molecular targets is the subject of intense investigation. The knowledge of all of the signal and receptor components potentially involved in the functional deregulation of vascular cells by oxidized lipid species will have a profound impact on understanding and modulation of atherogenesis.

The authors thank Mr. Stefan Weißgerber for exceptional help with image processing. The authors are grateful to Dr. Dieter F. Münzer for valuable assistance with the SYBYL software. The authors acknowledge financial support from the Austrian Science Fund (FWF projects P14714-PHA, P13962-CHE, and SFB F30-B05).

REFERENCES

1. Steinberg, D., S. Parthasarathy, T. E. Carew, J. C. Khoo, and J. L. Witztum. 1989. Beyond cholesterol. Modifications of low-density lipoprotein that increase its atherogenicity. *N. Engl. J. Med.* **320:** 915–924.
2. Witztum, J. L., and D. Steinberg. 1991. Role of oxidized low density lipoprotein in atherogenesis. *J. Clin. Invest.* **88:** 1785–1792.
3. Berliner, J. A., M. Navab, A. M. Fogelman, J. S. Frank, L. L. Demer, P. A. Edwards, A. D. Watson, and A. J. Lusis. 1995. Atherosclerosis. Basic mechanisms: oxidation, inflammation, and genetics. *Circulation.* **91:** 2488–2496.
4. Marathe, G. K., S. M. Prescott, G. A. Zimmerman, and T. M. McIntyre. 2001. Oxidized LDL contains inflammatory PAF-like phospholipids. *Trends Cardiovasc. Med.* **11:** 139–142.
5. Itabe, H., Y. Kushi, S. Handa, and K. Inoue. 1988. Identification of 2-azelaoylphosphatidylcholine as one of the cytotoxic products generated during oxyhemoglobin-induced peroxidation of phosphatidylcholine. *Biochim. Biophys. Acta.* **962:** 8–15.
6. Tanaka, T., H. Minamino, S. Unezaki, H. Tsukatani, and A. Tokumura. 1993. Formation of platelet-activating factor-like phospholipids by Fe^{2+}/ascorbate/EDTA-induced lipid peroxidation. *Biochim. Biophys. Acta.* **1166:** 264–274.
7. Leitinger, N., T. R. Tyner, L. Oslund, C. Rizza, G. Subbanagounder, H. Lee, P. T. Shih, N. Mackman, G. Tigyi, M. C. Territo, et al. 1999. Structurally similar oxidized phospholipids differentially regulate endothelial binding of monocytes and neutrophils. *Proc. Natl. Acad. Sci. USA.* **96:** 12010–12015.
8. Watson, A. D., M. Navab, S. Y. Hama, A. Sevanian, S. M. Prescott, D. M. Stafforini, T. M. McIntyre, B. N. Du, A. M. Fogelman, and J. A. Berliner. 1995. Effect of platelet activating factor-acetylhydrolase on the formation and action of minimally oxidized low density lipoprotein. *J. Clin. Invest.* **95:** 774–782.
9. Subbanagounder, G., N. Leitinger, D. C. Schwenke, J. W. Wong, H. Lee, C. Rizza, A. D. Watson, K. F. Faull, A. M. Fogelman, and J. A. Berliner. 2000. Determinants of bioactivity of oxidized phospholipids: specific oxidized fatty acyl groups at the sn-2 position. *Arterioscler. Thromb. Vasc. Biol.* **20:** 2248–2254.
10. Leitinger, N., A. D. Watson, K. F. Faull, A. M. Fogelman, and J. A. Berliner. 1997. Monocyte binding to endothelial cells induced by oxidized phospholipids present in minimally oxidized low density lipoprotein is inhibited by a platelet activating factor receptor antagonist. *Adv. Exp. Med. Biol.* **433:** 379–382.
11. Loidl, A., E. Sevcsik, G. Riesenhuber, H. P. Deigner, and A. Hermetter. 2003. Oxidized phospholipids in minimally modified low density lipoprotein induce apoptotic signaling via activation of acid sphingomyelinase in arterial smooth muscle cells. *J. Biol. Chem.* **278:** 32921–32928.
12. Watson, A. D., N. Leitinger, M. Navab, K. F. Faull, S. Horkko, J. L. Witztum, W. Palinski, D. Schwenke, R. G. Salomon, W. Sha, et al. 1997. Structural identification by mass spectrometry of oxidized phospholipids in minimally oxidized low density lipoprotein that induce monocyte/endothelial interactions and evidence for their presence in vivo. *J. Biol. Chem.* **272:** 13597–13607.
13. Itabe, H., E. Takeshima, H. Iwasaki, J. Kimura, Y. Yoshida, T. Imanaka, and T. Takano. 1994. A monoclonal antibody against oxidized lipoprotein recognizes foam cells in atherosclerotic lesions. Complex formation of oxidized phosphatidylcholines and polypeptides. *J. Biol. Chem.* **269:** 15274–15279.
14. Horkko, S., D. A. Bird, E. Miller, H. Itabe, N. Leitinger, G. Subbanagounder, J. A. Berliner, P. Friedman, E. A. Dennis, L. K. Curtiss, et al. 1999. Monoclonal autoantibodies specific for oxidized phospholipids or oxidized phospholipid-protein adducts inhibit macrophage uptake of oxidized low-density lipoproteins. *J. Clin. Invest.* **103:** 117–128.
15. Palinski, W., R. K. Tangirala, E. Miller, S. G. Young, and J. L. Witztum. 1995. Increased autoantibody titers against epitopes of oxidized LDL in LDL receptor-deficient mice with increased atherosclerosis. *Arterioscler. Thromb. Vasc. Biol.* **15:** 1569–1576.
16. Palinski, W., S. Horkko, E. Miller, U. P. Steinbrecher, H. C. Powell, L. K. Curtiss, and J. L. Witztum. 1996. Cloning of monoclonal autoantibodies to epitopes of oxidized lipoproteins from apolipoprotein E-deficient mice. Demonstration of epitopes of oxidized low density lipoprotein in human plasma. *J. Clin. Invest.* **98:** 800–814.
17. Kadl, A., J. Huber, F. Gruber, V. N. Bochkov, B. R. Binder, and N. Leitinger. 2002. Analysis of inflammatory gene induction by oxidized phospholipids in vivo by quantitative real-time RT-PCR in comparison with effects of LPS. *Vascul. Pharmacol.* **38:** 219–227.
18. Reddy, S., S. Hama, V. Grijalva, K. Hassan, R. Mottahedeh, G. Hough, D. J. Wadleigh, M. Navab, and A. M. Fogelman. 2001. Mitogen-activated protein kinase phosphatase 1 activity is necessary for oxidized phospholipids to induce monocyte chemotactic activity in human aortic endothelial cells. *J. Biol. Chem.* **276:** 17030–17035.
19. Walton, K. A., A. L. Cole, M. Yeh, G. Subbanagounder, S. R. Krutzik, R. L. Modlin, R. M. Lucas, J. Nakai, E. J. Smart, D. K. Vora, et al. 2003. Specific phospholipid oxidation products inhibit ligand activation of Toll-like receptors 4 and 2. *Arterioscler. Thromb. Vasc. Biol.* **23:** 1197–1203.
20. Ishikawa, K., M. Navab, N. Leitinger, A. M. Fogelman, and A. J. Lusis. 1997. Induction of heme oxygenase-1 inhibits the monocyte transmigration induced by mildly oxidized LDL. *J. Clin. Invest.* **100:** 1209–1216.
21. Owens, G. K. 1995. Regulation of differentiation of vascular smooth muscle cells. *Physiol. Rev.* **75:** 487–517.
22. Pauletto, P., R. Sarzani, A. Rappelli, A. Chiavegato, A. C. Pessina, and S. Sartore. 1994. Differentiation and growth of vascular smooth muscle cells in experimental hypertension. *Am. J. Hypertens.* **7:** 661–674.
23. Kogure, K., S. Nakashima, A. Tsuchie, A. Tokumura, and K. Fukuzawa. 2003. Temporary membrane distortion of vascular smooth muscle cells is responsible for their apoptosis induced by platelet-activating factor-like oxidized phospholipids and their degradation product, lysophosphatidylcholine. *Chem. Phys. Lipids.* **126:** 29–38.
24. Dittmer, J. C., and R. L. Lester. 1964. A simple, specific spray for the detection of phospholipids on thin-layer chromatograms. *J. Lipid Res.* **15:** 126–127.
25. Rouser, G., A. N. Siakotos, and S. Fleischer. 1966. Quantitative analysis of phospholipids by thin-layer chromatography and phosphorus analysis of spots. *Lipids.* **1:** 85–86.
26. Subbanagounder, G., A. D. Watson, and J. A. Berliner. 2000. Bioactive products of phospholipid oxidation: isolation, identification, measurement and activities. *Free Radic. Biol. Med.* **28:** 1751–1761.
27. Chung, B. H., T. Wilkinson, J. C. Geer, and J. P. Segrest. 1980. Preparative and quantitative isolation of plasma lipoproteins: rapid, single discontinuous density gradient ultracentrifugation in a vertical rotor. *J. Lipid Res.* **21:** 284–291.
28. Lowry, O. H., N. J. Rosebrough, A. L. Farr, and R. J. Randall. 1951. Protein measurement with the Folin phenol reagent. *J. Biol. Chem.* **193:** 265–275.

Downloaded from www.jlr.org by guest, on June 14, 2012

29. Hofer, G., E. Steyrer, G. M. Kostner, and A. Hermetter. 1997. LDL-mediated interaction of Lp[a] with HepG2 cells: a novel fluorescence microscopy approach. *J. Lipid Res.* **38:** 2411–2421.
30. Bradford, M. M. 1976. A rapid and sensitive method for the quantitation of microgram quantities of protein utilizing the principle of protein-dye binding. *Anal. Biochem.* **72:** 248–254.
31. Wessel, D., and U. I. Fluegge. 1984. A method for the quantitative recovery of protein in dilute solution in the presence of detergents and lipids. *Anal. Biochem.* **138:** 141–143.
32. Bjellqvist, B., K. Ek, P. G. Righetti, E. Gianazza, A. Görg, R. Westermeier, and W. Postel. 1982. Isoelectric focusing in immobilized pH gradients: principle, methodology and some applications. *J. Biochem. Biophys. Methods.* **6:** 317–339.
33. Bjellqvist, B., J-C. Sanchez, C. Pasquali, F. Ravier, N. Paquet, S. Frutiger, G. J. Hughes, and D. F. Hochstrasser. 1993. Micropreparative two-dimensional electrophoresis allowing separation of samples containing milligram amounts of protein. *Electrophoresis.* **14:** 1375–1378.
34. Sanchez, J-C., V. Rouge, M. Pisteur, F. Ravier, L. Tonella, M. Moosmayer, M. R. Wilkins, and D. F. Hochstrasser. 1997. Improved and simplified in-gel sample application using reswelling of dry immobilized pH gradients. *Electrophoresis.* **18:** 324–327.
35. Görg, A., W. Postel, S. Günther, and J. Weser. 1985. Improved horizontal two-dimensional electrophoresis with hybrid isoelectric focusing in immobilized pH gradients in the first dimension and laying-on transfer to the second dimension. *Electrophoresis.* **6:** 599–604.
36. Görg, A., W. Postel, and S. Günther. 1988. The current state of two-dimensional electrophoresis with immobilized pH gradients. *Electrophoresis.* **9:** 531–546.
37. Folch, J., M. Lees, and G. H. Sloane Stanley. 1957. A simple method for the isolation and purification of total lipids from animal tissues. *J. Biol. Chem.* **226:** 497–509.
38. Zieseniss, S., S. Zahler, I. Muller, A. Hermetter, and B. Engelmann. 2001. Modified phosphatidylethanolamine as the active component of oxidized low density lipoprotein promoting platelet prothrombinase activity. *J. Biol. Chem.* **276:** 19828–19835.
39. Friedman, P., S. Horkko, D. Steinberg, J. L. Witztum, and E. A. Dennis. 2002. Correlation of antiphospholipid antibody recognition with the structure of synthetic oxidized phospholipids. importance of Schiff base formation and aldol condensation. *J. Biol. Chem.* **277:** 7010–7020.
40. Kuhn, N., A. Kuhn, J. Lewandowski, and M. Speis. 1991. 1,2,3-Diazaborinium compounds—new cationic boron heteroarenes. *Chem. Ber.* **124:** 2197–2201.
41. Haugland, R. P. 1992. Handbook of Fluorescent Probes and Research Products. 5th edition. Molecular Probes, Inc., Eugene, OR.
42. Idziorek, T., J. Estaquier, F. De Bels, and J. C. Ameisen. 1995. YOPRO-1 permits cytofluorometric analysis of programmed cell death (apoptosis) without interfering with cell viability. *J. Immunol. Methods.* **185:** 249–258.
43. Cohen, J. J. 1993. Apoptosis. *Immunol. Today.* **14:** 126–130.
44. Foerster, T. 1969. Excimers. *Angew. Chem. Int. Ed. Engl.* **8:** 333–343.
45. Hazen, S. L., J. Heller, F-F. Hsu, A. d'Avignon, and J. W. Heinecke. 1999. Synthesis, isolation, and characterization of the adduct formed in the reaction of *p*-hydroxyphenylacetaldehyde with the amino headgroup of phosphatidylethanolamine and phosphatidylserine. *Chem. Res. Toxicol.* **12:** 19–27.
46. Naylor, B. L., M. Picardo, R. Homan, and H. J. Pownall. 1991. Effects of fluorophore structure and hydrophobicity on the uptake and metabolism of fluorescent lipid analogs. *Chem. Phys. Lipids.* **58:** 111–119.
46a. Fruhwirth, G. O., A. Moumtzi, A. Loidl, E. Ingolic, and A. Hermetter. 2006. The oxidized phospholipids POVPC and PGPC inhibit growth and induce apoptosis in vascular smooth muscle cells. *Biochim. Biophys. Acta.* **1761:** 1060–1069.
47. Struck, D. K., and R. E. Pagano. 1980. Insertion of fluorescent phospholipids into the plasma membrane of a mammalian cell. *J. Biol. Chem.* **255:** 5404–5410.
48. Nichols, J. W., and R. E. Pagano. 1981. Kinetics of soluble lipid monomer diffusion between vesicles. *Biochemistry.* **20:** 2783–2789.
49. Hamori, E., and A. M. Michaels. 1971. Determination of critical micelle concentration of aqueous lysolecithin solutions. *Biochim. Biophys. Acta.* **231:** 496–504.
50. Esterbauer, H., R. J. Schaur, and H. Zollner. 1991. Chemistry and biochemistry of 4-hydroxynonenal, malonaldehyde and related aldehydes. *Free Radic. Biol. Med.* **11:** 81–128.
51. Uchida, K., L. I. Szweda, H. Chae, and E. R. Stadtman. 1993. Immunochemical detection of 4-hydroxynonenal protein adducts in oxidized hepatocytes. *Proc. Natl. Acad. Sci. USA.* **90:** 8742–8746.
52. Liu, W., A. A. Akhand, M. Kato, I. Yokoyama, T. Miyata, K. Kurokawa, K. Uchida, and I. Nakashima. 1999. 4-Hydroxynonenal triggers an epidermal growth factor receptor-linked signal pathway for growth inhibition. *J. Cell Sci.* **112:** 2409–2417.
53. Suc, I., O. Meilhac, I. Lajoie-Mazenc, J. Vandaele, G. Jurgens, R. Salvayre, and A. Negre-Salvayre. 1998. Activation of EGF receptor by oxidized LDL. *FASEB J.* **12:** 665–671.
54. Gillotte, K. L., S. Horkko, J. L. Witztum, and D. Steinberg. 2000. Oxidized phospholipids, linked to apolipoprotein B of oxidized LDL, are ligands for macrophage scavenger receptors. *J. Lipid Res.* **41:** 824–833.
55. Brown, M. S., and J. L. Goldstein. 1997. The SREBP pathway: regulation of cholesterol metabolism by proteolysis of a membrane-bound transcription factor. *Cell.* **89:** 331–340.
56. Podrez, E. A., G. Hoppe, J. O'Neil, and H. F. Hoff. 2003. Phospholipids in oxidized LDL not adducted to apoB are recognized by the CD36 scavenger receptor. *Free Radic. Biol. Med.* **34:** 356–364.
57. Ahmed, Z., A. Ravandi, G. F. Maguire, A. Kuksis, and P. W. Connelly. 2003. Formation of apolipoprotein AI-phosphatidylcholine core aldehyde Schiff base adducts promotes uptake by THP-1 macrophages. *Cardiovasc. Res.* **58:** 712–720.
58. Anderson, R. G. W. 1998. The caveolae membrane system. *Annu. Rev. Biochem.* **67:** 199–225.
59. Kurzchalia, T. V., and R. G. Parton. 1999. Membrane microdomains and caveolae. *Curr. Opin. Cell Biol.* **11:** 424–431.
60. Tillman, T. S., and M. Cascio. 2003. Effects of membrane lipids on ion channel structure and function. *Cell Biochem. Biophys.* **38:** 161–190.
61. Simons, K., and G. van Meer. 1988. Lipid sorting in epithelial cells. *Biochemistry.* **27:** 6197–6202.
62. Simons, K., and E. Ikonen. 1997. Functional rafts in cell membranes. *Nature.* **387:** 569–572.
63. Walton, K. A., X. Hsieh, N. Gharavi, S. Wang, G. Wang, M. Yeh, A. L. Cole, and J. A. Berliner. 2003. Receptors involved in the oxidized 1-palmitoyl-2-arachidonoyl-sn-glycero-3-phosphorylcholine-mediated synthesis of interleukin-8: a role for Toll-like receptor 4 and a glycosylphosphatidylinositol-anchored protein. *J. Biol. Chem.* **278:** 29661–29666.
64. Navab, M., J. A. Berliner, G. Subbanagounder, S. Hama, A. J. Lusis, L. W. Castellani, S. Reddy, D. Shih, W. Shi, A. D. Watson, et al. 2001. HDL and the inflammatory response induced by LDL-derived oxidized phospholipids. *Arterioscler. Thromb. Vasc. Biol.* **21:** 481–488.
65. Heery, J. M., M. Kozak, D. M. Stafforini, D. A. Jones, G. A. Zimmerman, T. M. McIntyre, and S. M. Prescott. 1995. Oxidatively modified LDL contains phospholipids with platelet-activating factor-like activity and stimulates the growth of smooth muscle cells. *J. Clin. Invest.* **96:** 2322–2330.
66. Kern, H., T. Volk, S. Knauer-Schiefer, T. Mieth, B. Rustow, W. J. Kox, and M. Schlame. 1998. Stimulation of monocytes and platelets by short-chain phosphatidylcholines with and without terminal carboxyl group. *Biochim. Biophys. Acta.* **1394:** 33–42.
67. Smiley, P. L., K. E. Stremler, S. M. Prescott, G. A. Zimmerman, and T. M. McIntyre. 1991. Oxidatively fragmented phosphatidylcholines activate human neutrophils through the receptor for platelet-activating factor. *J. Biol. Chem.* **266:** 11104–11110.
68. Subbanagounder, G., N. Leitinger, P. T. Shih, K. F. Faull, and J. A. Berliner. 1999. Evidence that phospholipid oxidation products and/or platelet-activating factor play an important role in early atherogenesis: in vitro and in vivo inhibition by WEB 2086. *Circ. Res.* **85:** 311–318.
69. Watson, A. D., G. Subbanagounder, D. S. Welsbie, K. F. Faull, M. Navab, M. E. Jung, A. M. Fogelman, and J. A. Berliner. 1999. Structural identification of a novel pro-inflammatory epoxyisoprostane phospholipid in mildly oxidized low density lipoprotein. *J. Biol. Chem.* **274:** 24787–24798.

Downloaded from www.jlr.org by guest, on June 14, 2012